Marine and Petroleum Geology 140 (2022) 105664

Contents lists available at ScienceDirect

Marine and Petroleum Geology

journal homepage: www.elsevier.com/locate/marpetgeo

Tracing Lower Cretaceous organic-rich units across the SW Barents Shelf

A. Hagset [a,*], S.-A. Grundvåg [a,b], B. Badics [c], R. Davies [c], A. Rotevatn [d]

[a] Department of Geosciences, UIT the Arctic University of Norway, Tromsø, Norway
[b] Department of Arctic Geology, University Centre in Svalbard, PO Box 156, N-9171, Longyearbyen, Norway
[c] Wintershall DEA, Stavanger, Norway
[d] Department of Geosciences, University of Bergen, Bergen, Norway

ARTICLE INFO

Keywords:
Lower Cretaceous stratigraphy
SW Barents Shelf
Source rock evaluation
Seismic attributes
Rock-Eval data analysis
Wireline logs
Source rock characteristics
Fault-bounded depocenters

ABSTRACT

On the Barents Shelf, the northernmost and least explored hydrocarbon province of the Norwegian Continental Shelf, Upper Jurassic organic-rich shales have traditionally been given most attention as these represent the most prolific source rock unit of the region. However, in the western frontier areas of the Barents Shelf, the Upper Jurassic is too deeply buried. By combining high-resolution 2D seismic data, well logs, and digitalized Rock-Eval data, this study documents the lateral distribution and variability of alternative source rock units within the Lower Cretaceous succession on the SW Barents Shelf. Negative high-amplitude anomalies are traced from shallow basins on the platform westward into deeper basins along the western shelf margin. The anomalies are tied to intervals of increased total organic carbon contents in several exploration wells, and we thus establish the presence of four potential source rock units; these are the (1) upper Hauterivian, (2) Barremian, (3) lower Aptian, and (4) upper Cenomanian units. Based on the distribution of the associated seismic anomalies, we infer that the deposition and preservation of these organic-rich units are coupled to localized, fault bounded depocenters, mainly controlled by Late Jurassic – Early Cretaceous rifting and local reactivation events. The lower Aptian stands out as the most significant source rock unit, particularly in the Fingerdjupet Subbasin, where it displays a kerogen Type II composition. The distribution and development of this oil-prone source rock unit is linked to an early Aptian fault reactivation event. Due to increased sediment influx in combination with high subsidence rates during the Albian to Cenomanian, potential pre-Aptian source rock units appear to have undergone too deep burial in the Tromsø and Bjørnøya basins to be presently generative. Furthermore, organic matter dilution due to increased sedimentation rates seems to have reduced the overall potential of the upper Cenomanian unit.

1. Introduction

The presence of a thermally mature and viable source rock unit is one of the key risk factors in oil and gas exploration (White, 1993; Katz, 2005). Several factors may influence the development of a potential source rock unit, including primary organic production, preservation environment, and sedimentation rate (Pedersen and Calvert, 1990; Arthur et al., 1994; Calvert et al., 1996; Bohacs et al., 2005; Katz, 2005). In addition, the tectonic setting of a basin may represent an important first-order control on processes such as accommodation development (e.g. subsidence and burial) and water mass circulation that are vital for source rock development (Demaison et al., 1983; Gawthorpe et al., 2000). Across the Norwegian Continental Shelf (NCS), Upper Jurassic organic-rich shales have traditionally been given the most attention, as these represent the main source rock unit charging most of the largest producing oil and gas fields (Demaison et al., 1983; Cooper et al., 1984; Isaksen et al., 2001; Marín et al., 2020). This has left alternative source rock units to be considered as insignificant or even neglected (Ohm et al., 2008). This is also the case for the Barents Shelf, the northernmost and least explored hydrocarbon province of the NCS. Across large parts of the NCS, the widely distributed Upper Jurassic source rock unit was generally deposited during a period characterized by active faulting forming structurally restricted basins that were ideal sites for the accumulation and preservation of organic matter (e.g. Faleide et al., 1984; Leith et al., 1993; Jongepier et al., 1996; Langrock et al., 2003; Marín et al., 2020). However, despite its extensive distribution across the SW Barents Shelf, the traditional Upper Jurassic source rock unit only appears to be mature in a narrow belt along the western margin of the Hammerfest Basin and on the margins of the Loppa High (Dore, 1995; Marín et al., 2020). In the deeper marginal basins further to the

* Corresponding author.
E-mail address: aha155@uit.no (A. Hagset).

https://doi.org/10.1016/j.marpetgeo.2022.105664
Received 14 January 2022; Received in revised form 22 March 2022; Accepted 23 March 2022
Available online 28 March 2022

west, the Upper Jurassic source rock unit has been buried very deeply and is over-mature (Ohm et al., 2008). Documenting the presence of alternative source rock units at stratigraphic shallower intervals is, therefore, crucial for exploration success in these frontier areas.

Such alternative source rock units may occur in the Lower Cretaceous and Paleogene successions (Leith et al., 1993; Øygard and Olsen, 2002; Seldal, 2005; Lerch et al., 2017; Sattar et al., 2017). Several exploration wells have confirmed the presence of Lower Cretaceous source rock units in the Fingerdjupet Subbasin (e.g. 7321/9–1) and in the western part of the Hammerfest Basin (e.g. 7120/6-3 S) (NPD Factpages, 2021). Moreover, some petroleum discoveries have previously been linked to Lower Cretaceous source rocks by biomarkers (e.g. wells 7120/10–1, 7120/1–2, 7120/2-3 S, 6706/12–2, 6305/8–1, and 6405/7) (Lerch et al., 2017; NPD Factpages, 2021), and on the Mid-Norwegian Shelf are several oil discoveries identified as sourced by Cretaceous source rocks (Matapour and Karlsen, 2017). A regionally extensive, gas condensate-prone source rock unit of early Aptian age have been identified onshore Svalbard at the northwestern corner of the Barents Shelf (Midtkandal et al., 2016; Grundvåg et al., 2019). In addition, oil stains discovered in sandstones onshore northeastern Greenland indicate the presence of a Cretaceous-age source rock (Bojesen-Koefoed et al., 2020). However, there are large uncertainties

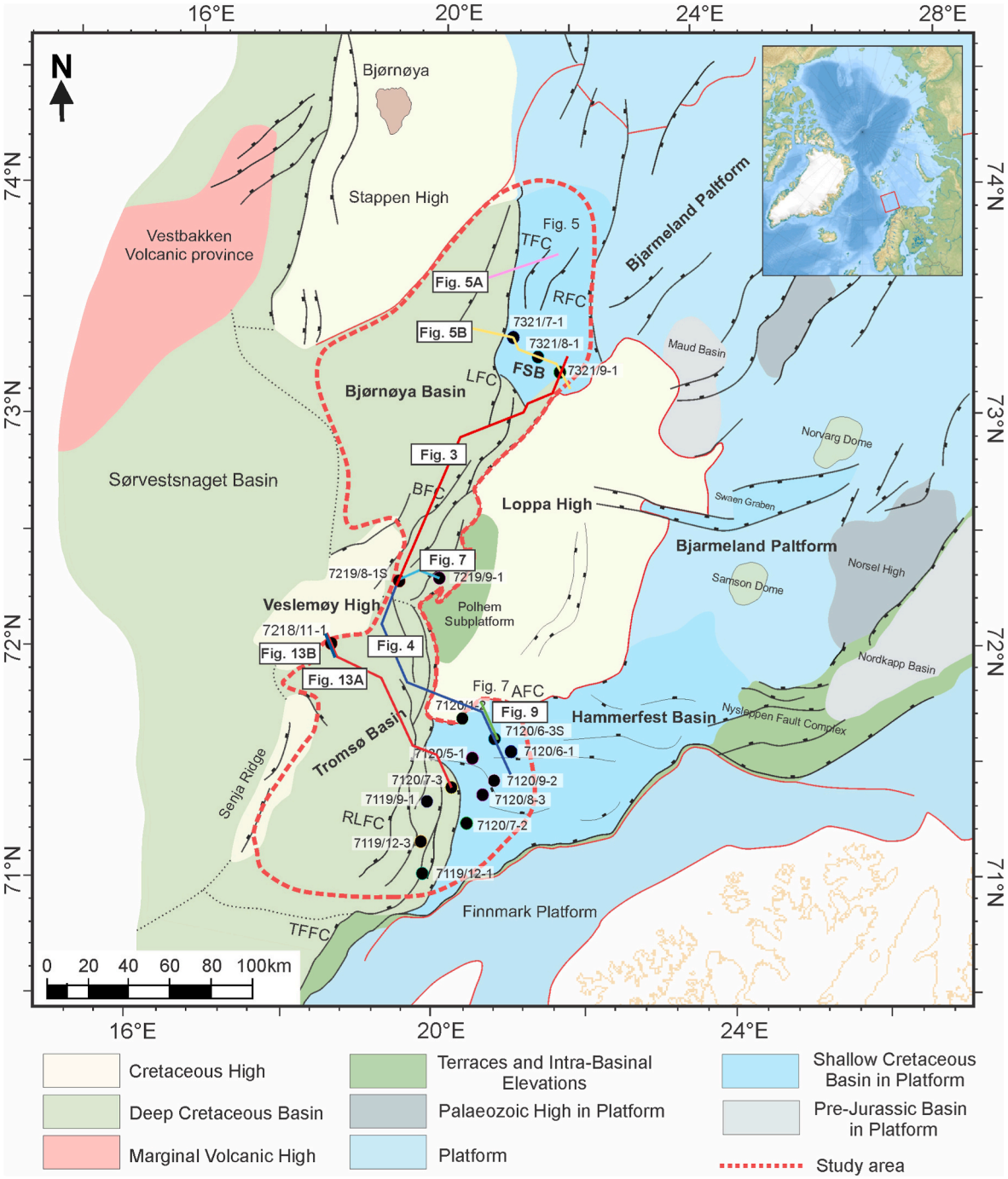

Fig. 1. Structural map of the SW Barents Shelf. The study area includes the western part of the Hammerfest Basin, the Tromsø Basin, the Bjørnøya Basin and the Fingerdjupet Subbasin. Key wells and seismic lines are annotated. TFFC: Troms Finnmark Fault Complex, RLFC: Ringvassøy Loppa Fault Complex, BFC: Bjørnøyrenna Fault Complex, AFC: Asterias Fault Complex, FSB: Fingerdjupet Subbasin, LFC: Leirdjupet Fault Complex, RFS: Randi Fault Set. Modified after NPD Factpages (2021).

related to the presence, stratigraphic position, and lateral distribution of Lower Cretaceous source rock units offshore, particularly in the deep basins along the western shelf margin. The regional significance of Lower Cretaceous source rocks is, therefore, still largely unclear (Dore, 1995; Mann et al., 2002; Øygard and Olsen, 2002; Seldal, 2005; Lerch et al., 2017). Thus, a detailed investigation of organic-rich units exhibiting source rock potential within the Lower Cretaceous succession seems essential in developing new play models and reducing exploration risk in the western frontier areas of the Barents Shelf.

By combining high-resolution regional 2D seismic data, well logs, and a digitalized Rock-Eval database, this study documents the lateral and stratigraphic distribution and variability of potential source rock units within the Lower Cretaceous succession on the southwestern Barents Shelf (Fig. 1). In particular, this study applies traditional source rock evaluation methods (sensu Peters and Cassa, 1994) to establish the potential and quality of the recognized potential source rock units in the shallow basins located on the interior platform part of the shelf (e.g. the Fingerdjupet Subbasin and Hammerfest Basin). This analysis will further aid in mapping the lateral and stratigraphic distribution of potential source rock units in the deeper marginal basins (e.g. the Tromsø and Bjørnøya basins). Finally, various factors that controlled the development and distribution of the investigated organic-rich intervals, such as the tectono-sedimentary evolution of the various basins, are evaluated and discussed.

2. Geological framework

2.1. Structural setting

The Barents Shelf is an epicontinental platform situated between the Norwegian mainland in the south, the Svalbard archipelago and Franz Josef Land to the north, and Novaya Zemlya to the east/southeast (Fig. 1). Following the Caledonian orogeny in the Late Silurian – Early Devonian, the shelf has undergone multiple phases of extension and subordinate compression, which have resulted in a complex pattern of fault-bounded basins and highs, as well as platform areas and smaller inversion-related structures (Faleide et al., 1984, 1993a, 1993b, 2008; Riis et al., 2014). The main extensional, basin-forming phases occurred during i) the Late Devonian associated with the collapse of the Caledonian orogenic belt, ii) the Late Carboniferous, iii) the Late Permian – Early Triassic, iv) the Late Jurassic – Early Cretaceous, and v) finally during the complete opening of the NE Atlantic rift system during the Late Cretaceous – Early Paleogene (Faleide et al., 2008, 2015).

The most important basins for this study include: 1) the Fingerdjupet Subbasin; 2) the Bjørnøya Basin; 3) Hammerfest Basin; and 4) the Tromsø Basin (Fig. 1). In general, the evolution of these basins is related to the Late Jurassic – Early Cretaceous extensional event. A brief outline of their structural development is given below.

2.1.1. Fingerdjupet Subbasin

The Fingerdjupet Subbasin is considered to be the shallow northeastern extension of the Bjørnøya Basin. Its southern and western boundaries are defined by the Leirdjupet Fault Complex (LFC) (Gabrielsen et al., 1990; Faleide et al., 1993a), whereas the Bjarmeland Platform and the Loppa High defines its eastern and southeastern boundaries (Gabrielsen et al., 1990, Fig. 1). The Fingerdjupet Subbasin is characterized by a horst and graben configuration, with a series of faults that developed during Late Jurassic extension and local reactivation during the Early Cretaceous (Faleide et al., 1993b). This includes the Randi Fault Set (RFS), situated in the eastern transition to the Bjarmeland Platform (Serck et al., 2017). Furthermore, an Aptian extensional event is well documented in the Fingerdjupet Subbasin (Faleide et al., 1993a; Clark et al., 2014; Blaich et al., 2017; Serck et al., 2017). This fault activity initiated the formation of localized wedges and contributed to the uplift of the northern parts of Loppa High (Indrevær et al., 2017; Marín et al., 2017). Because of Cenozoic uplift and erosion (Henriksen et al., 2011; Lasabuda et al., 2018, 2021) only the lowermost part of the Lower Cretaceous succession is preserved in the basin.

2.1.2. Bjørnøya Basin

The NE–SW-oriented Bjørnøya Basin is bounded by the LFC to the east, by the Bjørnøyrenna Fault Complex (BFC) to the southeast, and by the faulted margin of the Stappen High to the northwest (Fig. 1), cf. Gabrielsen et al. (1990). Structuring of the Bjørnøya Basin is also attributed to the Late Jurassic – Early Cretaceous extensional event (Faleide et al., 1993a, 1993b). Consequently, most of the basin infill is of Early Cretaceous age (Gabrielsen et al., 1990; Faleide et al., 1993a). The basin was affected by faulting and local inversion in association with the BFC and uplift of the Stappen High during the Late Cretaceous and Paleogene (Faleide et al., 1993a).

2.1.3. Hammerfest Basin

The Hammerfest Basin is an elongated ENE – WSW oriented basin, located south of the Loppa High (Fig. 1). The Ringvassøy-Loppa Fault Complex (RLFC) separates it from the deeper Tromsø Basin to the west, while the Asterias Fault complex (AFC) separates it from the Loppa High (Gabrielsen et al., 1990). Its southern border is defined by the Troms-Finnmark Fault Complex (TFFC), which separates the basin from the Finnmark Platform (Gabrielsen et al., 1990). Structuring of the Hammerfest Basin is mainly attributed to extension in Triassic and Late Jurassic to Early Cretaceous times (Berglund et al., 1986; Gabrielsen et al., 1990; Faleide et al., 1993a). Local compression has also been documented (Sund, 1984; Gabrielsen et al., 1997; Indrevær et al., 2017). Uplift and doming along the central basin axis started in the Middle Jurassic (Berglund et al., 1986) and extended into the Early Cretaceous (Berglund et al., 1986; Faleide et al., 1993a). Consequently, new depocenters formed along the boundaries of the Hammerfest Basin (Marín et al., 2017). The uplift ceased in the early Barremian (Faleide et al., 1993a), leaving most of the Barremian – Aptian succession confined within the faulted boundaries of the basin (Marín et al., 2017, 2018b).

2.1.4. Tromsø Basin

The Tromsø Basin is an NNE – SSW-oriented basin that transitions southwards into the Harstad Basin, eventually terminating against the TFFC (Fig. 1). The BFC and the Veslemøy High define its northern boundary, separating it from the Bjørnøya Basin. The RLFC delineates the eastern boundary towards the Hammerfest Basin, while the Senja Ridge marks its western boundary (Gabrielsen et al., 1990). As the North Atlantic rift system advanced northward during the Middle Jurassic – Early Cretaceous, deep basins formed along the southwestern Barents Shelf margin (Faleide et al., 1993a, 1993b). The Early Cretaceous extensional event in the Tromsø Basin was focused along the NE-SW trending RLFC and the BFC. Consequently, the Tromsø Basin experienced rapid subsidence, creating immense accommodation space for Cretaceous sediments, preserved as an up to ca. 8 km thick succession (Rønnevik et al., 1982; Gabrielsen et al., 1990; Faleide et al., 1993a, 2008; Clark et al., 2014; Indrevær et al., 2017; Kairanov et al., 2021). A total of three Early Cretaceous extensional phases have been documented for the Tromsø Basin (Berriasian – Valanginian, Hauterivian – Barremian and Aptian – Albian) (Faleide et al., 1993a; Kairanov et al., 2021). In addition, Late Palaeozoic salt deposits were mobilized by rapid subsidence and differential loading during Albian times, triggering

diapirism in the central parts of the basin (Kairanov et al., 2021).

2.2. Lower Cretaceous stratigraphy and depositional systems

The Lower Cretaceous succession on the Barents Shelf is divided into the Knurr (Berriasian – Early Barremian), Klippfisk (Late Berriasian – Hauterivian), Kolje (Barremian – Early Aptian) and Kolmule (Aptian – Cenomanian) Formations (Fig. 2), collectively assigned to the Adventdalen Group (Parker, 1967; Dalland et al., 1988). Because there are some age-related uncertainties in correlating these units across the various basins, the Lower Cretaceous succession was recently subdivided into seven genetic sequences (S0 – S6; Fig. 2) bounded by regionally extensive flooding surfaces (Marín et al., 2017). Sequences S0 and S1 corresponds to the Knurr and Klippfisk formations, whereas sequence S2 correspond roughly to the Kolje Formation, and sequences S3 to S6 represents the Kolmule Formation (Marín et al., 2017, Fig. 2).

On the SW Barents Shelf, the Lower Cretaceous succession was generally deposited in open marine shelf environments, affected by periods of restricted bottom circulation (Dalland et al., 1988). The dominant lithology of the succession is grey-brown mudstones with interbeds of siltstone, limestone, and local sandstones (e.g. Worsley et al., 1988; Bugge et al., 2002; Seldal, 2005). The up to 285 m thick (as measured in well 7120/12–1) mudstone-dominated Knurr Formation (Valanginian–early Barremian), and the laterally equivalent carbonate-dominated Klippfisk Formation (Valanginian–Hauterivian) on the eastern platform areas constitute the lowermost part of the Lower Cretaceous succession (Dalland et al., 1988; Smelror et al., 1998). These are both condensed units containing multiple stratigraphic gaps (Smelror et al., 2009). Sandstone units emplaced by gravity-flow process occur locally near structural highs (Seldal, 2005; Sattar et al., 2017; Marín et al., 2018a).

The up to 437 m thick (as measured in well 7119/12–1) mudstone-dominated Kolje Formation (Barremian – earliest Aptian) was deposited in a shelf setting under generally well-oxygenated, open marine conditions (Dalland et al., 1988). A large-scale delta system prograding from the NW, reached the Fingerdjupet Subbasin in Barremian – Aptian times, as evident by the presence of several clinoform-bearing sequences in the upper part of the Barremian succession (Grundvåg et al., 2017; Marín et al., 2017; Midtkandal et al., 2019). A regionally extensive flooding surface, which caps the clinoforms, separates the Kolje Formation from the overlying Kolmule Formation (Grundvåg et al., 2017; Serck et al., 2017; Marín et al., 2018b).

The up to 950 m thick (as measured in well 7119/12–1) mudstone-rich and sandstone-bearing Kolmule Formation (Aptian–Middle Cenomanian) was deposited in response to significant uplift of the northeastern Barents Shelf, particularly during the Albian. Large amounts of sediments were shed off uplifted terranes and transported towards the rapidly subsiding basins along the southwestern shelf margin, such as the Harstad, Tromsø and Bjørnøya basins (Faleide et al., 1993a, 1993b; Smelror et al., 2009). Consequently, a large delta system prograded from the E to NE onto the SW Barents Shelf in the Aptian – Cenomanian (Grundvåg et al., 2017; Marín et al., 2017; Midtkandal et al., 2019). At these times, the shelf was generally characterized by well-oxygenated, open marine conditions (Smelror et al., 2009).

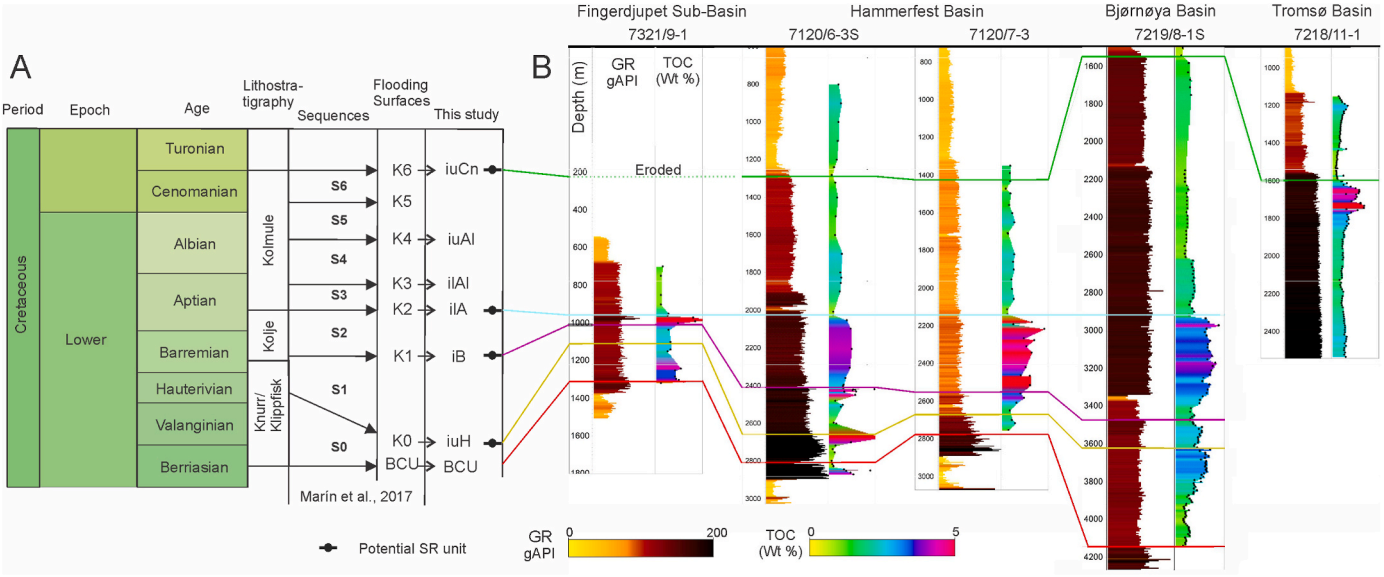

Fig. 2. (A) Lithostratigraphic overview of the Lower Cretaceous succession on the SW Barents Shelf. Marín et al. (2017) subdivided the succession into seven genetic sequences (S0 to S6) bounded by regionally extensive flooding surfaces (K0 to K6). This study conform to this sequence stratigraphic framework, but applies its own nomenclature for the flooding surfaces which refer more accurately to their stratigraphic position (similar to the naming convention of Serck et al., 2017). The chronostratigraphic chart has been modified after Cohen et al. (2013). (B) Correlation of four selected wells showing the distribution of the sequences and the extent of the flooding surfaces across the study area. In this study, four of the flooding surfaces are linked to potential source rock units (marked by source rock symbol in Fig. 2A), which are associated with increased total organic carbon (TOC) contents in the wells. The TOC logs are based on Rock-Eval data from either sidewall cores or drill cuttings. Well locations is displayed in Fig. 1. Abbreviations: iuCn: intra upper Cenomanian, iuAl: intra upper Albian, ilAl: intra lower Albian, ilA: intra lower Aptian, iB: intra Barremian, iuH: intra upper Hauterivian, BCU: Base Cretaceous Unconformity (which defines the base of the entire succession), GR: Gamma ray.

3. Data and methods

3.1. Seismic data

This study includes several high-resolution regional 2D seismic surveys (NBR, 2006–2012). The different orientation and spacing (1–8 km) of the 2D lines make up a grid that spans the study area, thus forming a regional pseudo 3D-grid. The acquisition of these surveys took place over a period of several years, resulting in varying quality between the surveys. In general, frequencies are in the range of 10–50 Hz, while the polarity convention for the dataset is zero-phase normal polarity, following the nomenclature of Sheriff (2002). The description of reflection configurations and seismic geometries follow the terminology established by Mitchum et al. (1977).

Confidence of the seismic interpretations within the deeper basins is strongly affected by a decreasing seismic quality with depth. In addition, no well data were available for either the central parts of the Tromsø or the Bjørnøya basins.

3.1.1. Seismic response to organic-rich intervals and mapping of potential source rock units

Mudrocks with total organic carbon (TOC) contents >3 – 4% typically have significantly lower acoustic impedance and higher intrinsic anisotropy than mudrocks with lower amounts of organic content. The general density of kerogen is typical in the range of 1.1–1.4 g/cm^3, while mudrocks generally have a density of 2.7 g/cm^3 (Løseth et al., 2011; Rider and Kennedy, 2011). Organic matter will, therefore, influence the seismic response trough compressional velocity (Vp), shear velocity (Vs), bulk density, anisotropy, and attenuation (Løseth et al., 2011). A potential source rock unit may thus result in a high amplitude reflection characterized by a negative top and a positive base (Løseth et al., 2011). Furthermore, the acoustic impedance contrast is relatively stable down to a depth of c. 4500 m and decreases nonlinearly with increasing TOC content (Løseth et al., 2011). This has clear implications for the Lower Cretaceous succession, which is buried at depths down to 5–7 s two-way-travel time, in the deep Bjørnøya and Tromsø basins (Gabrielsen et al., 1990; Kairanov et al., 2021).

The seismic mapping thus specifically targets the top of potential source rock units as these are displayed as negative high-amplitude anomalies in the data. Biostratigraphic age determination of the mapped reflectors are guided by well tops from the publicly available database of the Norwegian Petroleum Directorate (NPD Factpages, 2021) and from in-house data provided by Wintershall-Dea Norway. In the deep Tromsø and Bjørnøya basins, well 7219/8-1 S is a key reference point in providing age-control of the Lower Cretaceous succession. In most cases, the targeted reflectors seem to correspond to regionally extensive maximum flooding surfaces documented by previous studies (e.g. Marín et al., 2017). Thus, for regional stratigraphic context, the genetic sequence subdivision of Marín et al. (2017, 2018a, 2018b), and partly that of Serck et al. (2017), is used for guidance in the Hammerfest Basin and Fingerdjupet Subbasin, respectively (with some minor modifications). In the Bjørnøya Basin, the stratigraphic subdivision builds largely on that of the Fingerdjupet Subbasin by correlating the seismic horizons across the LFC and TFC (Fig. 1). In the Tromsø Basin, the stratigraphic framework used in this study, builds largely on the recent work of Kairanov et al. (2021), and by linking it to the stratigraphic framework established by Marín et al. (2017) for the Hammerfest Basin.

To investigate lateral variability and distribution of potential source rock units, average negative amplitude maps have been generated for two of the high-amplitude reflectors following the workflow of Løseth et al. (2011). The negative amplitude map is not very reliable in the deep basins because of deteriorating seismic quality and reflector dimming, making a lateral correlation from the shallow basins a difficult and time-consuming task. Consequently, amplitude maps have only been generated for two of the mapped reflectors. The generation of the amplitude map uses a search window of 5 ms above and 20 ms below the interpretation of the reflector.

3.2. Well data

Seventeen exploration wells have been selected and investigated for this study (Fig. 1 and Table 1). All the wells have an established time-depth relationship trough calibration of check shots. Most of the wells exhibit a common suite of wireline-logs including gamma ray (GR), sonic (AC/DT), density (DEN), and deep resistivity (RDEP). Wireline logs are generally regarded to be a good supplement to seismic data when evaluating the presence of potential source rock units, Thus, to confirm the presence of potential source rock units mapped in the seismic data, wireline log signals are integrated with digitalized TOC logs derived from the Rock-Eval data. The thicknesses of the potential source rock units are estimated from the wireline data and subsequently, TOC samples within the interval, or from stratigraphically nearby intervals, are evaluated (Table 1). The typical wireline response to organic rich units is briefly outlined below.

Table 1
Overview of sample intervals and thickness of units sampled for total organic carbon (TOC) contents and Rock-Eval data. Intervals with no data are marked with "No samples" and the stratigraphically/spatially closest sample points have been used when applicable. Intervals with no potential source rock unit is marked with "N/A".

Exploration wells	Hauterivian sample interval and thickness	Barremian sample Interval and thickness	Lower Aptian sample Interval and thickness	Cenomanian sample interval and thickness
7321/7-1	1498–1520 m (22 m)	1328–1348 m (20 m)	1060–1112 m (52 m)	N/A
7321/8-1	1250–1289 m (39 m)	N/A	859–861 m (2 m)	N/A
7321/9-1	1103–1114 m (11 m)	N/A	961–985 m (24 m)	N/A
7219/8-1 S	3619–3751 m (132 m)	3469–3548 m (79 m)	2929–3088 m (159 m)	1573–1616 m (43 m)
7219/9-1	N/A	N/A	N/A	1467–1599 m (132 m)
7218/11-1	N/A	N/A	N/A	1626–1747 m (121 m)
7120/1-2	N/A	N/A	1815–1825 m (10 m)	N/A
7120/6-3 S	2662–2686 m (24 m)	2403–2451 m (48 m)	2032–2084 m (52 m)	1303–1346 m (43 m)
7120/6-1	2204–2226 m (22 m)	2063–2106 m (43 m)	1912–1953 m (41 m)	N/A
7120/9-2	1870–1880 m (10 m)	1770–1809 m (39 m)	1647–1693 m (46 m)	N/A
7120/8-3	2052–2070 m (18 m)	1960–1988 m (28 m)	1749–1806 m (57 m)	1121–1174 m (53 m)
				No samples
7120/7-2	1986–2002 m (16 m)	1939–1970 m (31 m)	1782–1835 m (53 m)	1067–1096 m (29 m)
7120/5-1	N/A	2148–2170 m (22 m)	N/A	N/A
7120/7-3	2699–2720 m (21 m)	2561–2580 m (19 m)	2142–2283 m (141 m)	1423–1474 m (51 m)
7119/9-1	2647–2656 m (9 m)	2526–2559 m (33 m)	2257–2370 m (113 m)	1562–1587 m (25 m)
7119/12-3	2954–2976 m (22 m)	2738–2768 m (30 m)	2378–2446 m (68 m)	1670–1707 m (37 m)
7119/12-1	2437–2461 m (24 m)	2282–2327 m (45 m)	1909–1992 m (83 m)	1050–1094 m (44 m)

3.2.1. Wireline responses to organic-rich units

3.2.1.1. Gamma ray log (GR). Organic-rich mudrocks commonly show high GR values because of elevated concentrations of uranium. However, this is not always the case as uranium can be a highly mobile element under the right conditions (Bowker and Grace, 2010; Helleren et al., 2020). In addition, the GR-signal may be subject to various interference from the well casing.

3.2.1.2. Sonic log (AC/DT). The presence of organic matter in mudrocks will lower the sonic travel time (Rider and Kennedy, 2011). This response is evidently more apparent in mature source rocks. However, using the sonic log independently to identify organic rich intervals is problematic, because it is impossible to separate low sonic values caused by the presence of organic matter from low sonic values caused by porosity changes (Rider and Kennedy, 2011).

3.2.1.3. Resistivity log (RDEP). The resistivity logs response to a source rock depends on the maturity of the organic matter (Rider and Kennedy, 2011). In immature organic matter, the response will be small due to high conductivity. In mature source rocks where, free petroleum are present in voids and fractures, the resistivity will increase significantly (Rider and Kennedy, 2011).

3.2.1.4. Density log (DEN). Mudrocks containing low amounts of organic matter have a higher density matrix (2.67 – 2.72 g/cm^3) compared to pure organic matter (1.1 – 1.2 g/cm^3). The density log will consequently read lower values in organic rich mudrocks (Rider and Kennedy, 2011). The presence of organic matter thus has a distinct effect on the overall mudrock density, which also shifts the acoustic impedance in the seismic data towards negative amplitudes (Løseth et al., 2011).

3.3. Rock-Eval data

In order to establish the richness, type, and thermal maturity of the source rock units identified in the seismic and wireline data, traditional source rock evaluation following the principles of Espitalié et al. (1977), Peters (1986) and Peters and Cassa (1994) are used. The Rock-Eval data presented here are based on samples derived from either sidewall cores or drill cuttings from the 17 wells. The sample spacing varies between each well (ranging from samples collected every 2–100 m; see Table 1 for sampling interval details), which consequently makes it difficult to achieve a good representation of thin source rock units occurring between the sampled intervals. In these cases, the nearest samples to the interval have been used where applicable. To establish the thermal maturity of the potential source rock units, emphasis has been given to T_{max} values as these are numerous throughout the dataset, while the scarce vitrinite reflectance (R_o) data supplement the interpretation when applicable.

The Rock-Eval database has been digitalized and implemented into Petrel for each corresponding well. This makes it possible for a direct correlation between the source rock reflections and the Rock-Eval data at any of the well locations. The complete Rock-Eval database, including TOC content, is given in the online supplementary file SF1.

4. Results

4.1. Seismic sequences and bounding surfaces

Seven genetic sequences (S0 – S6) and their bounding surfaces (i.e., the BCU, iuH, iB, ilA, ilAl, iuAl, IuCn reflectors of this study, see detailed descriptions below) are recognized within the Lower Cretaceous succession in the study area (Figs. 3 and 4), conforming to the well-established sequence stratigraphic framework of Marín et al. (2017, 2018a, 2018b). Thus, apart from the Base Cretaceous Unconformity (BCU), which defines the base of the Lower Cretaceous succession, the sequence-bounding surfaces represent regionally extensive maximum flooding surfaces that may be correlated from the Hammerfest Basin and the Fingerdjupet Subbasin westward into the Tromsø and Bjørnøya basins (Figs. 3 and 4; Marín et al., 2017). Bellow follows a seismic description of the genetic sequences and their bounding surfaces.

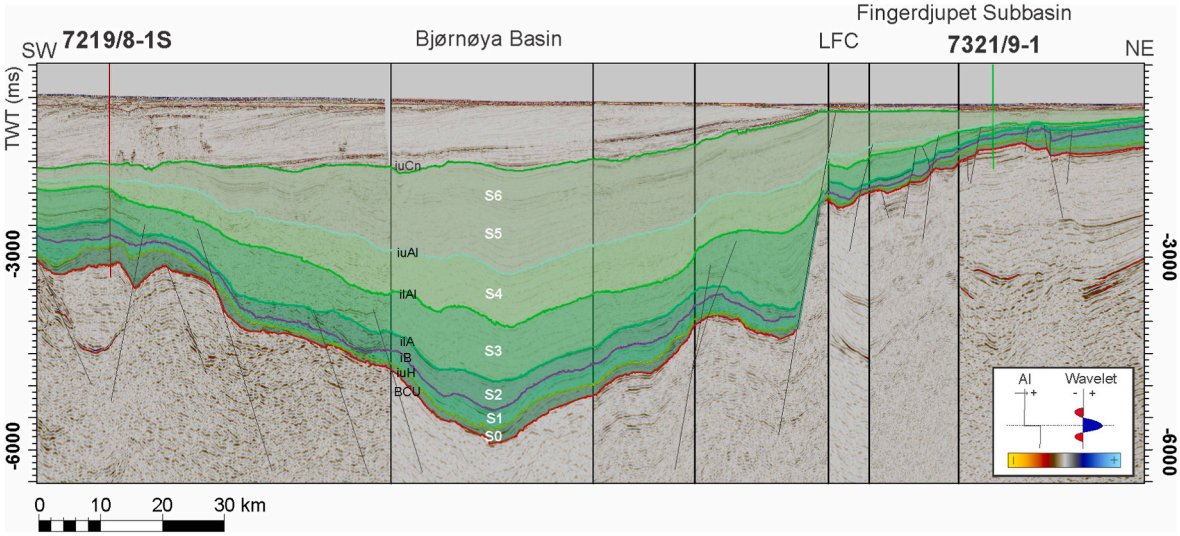

Fig. 3. Interpreted composite seismic line of the southern parts of Fingerdjupet Subbasin and the NE Bjørnøya Basin showing the seven genetic sequences comprising the Lower Cretaceous succession (S0 – S6; see Fig. 2). Location and orientation of the seismic line is shown in Fig. 1. Abbreviations: iuAl: intra upper Albian, ilAl: intra lower Albian, ilA: intra lower Aptian, iB: intra Barremian, iuH: intra upper Hauterivian, BCU: Base Cretaceous Unconformity. Seismic data courtesy TGS and Spectrum.

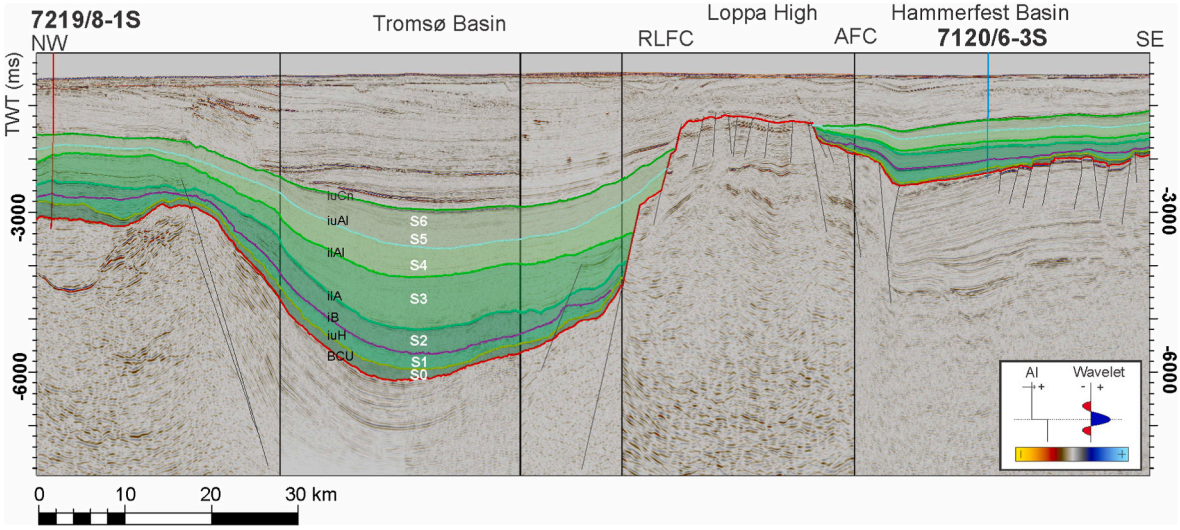

Fig. 4. Interpreted composite seismic line of the Tromsø Basin and the NW corner of the Hammerfest Basin, showing the seven genetic sequences comprising the Lower Cretaceous succession (S0 – S6; see Fig. 2). Location and orientation of the seismic line is shown in Fig. 1. Abbreviations: iuAl: intra upper Albian, ilAl: intra lower Albian, ilA: intra lower Aptian, iB: intra Barremian, iuH: intra upper Hauterivian, BCU: Base Cretaceous Unconformity. Seismic data courtesy TGS and Spectrum.

4.1.1. Sequence 0 (Berriasian – Hauterivian)

Sequence 0 is bounded at the base by the regionally extensive BCU, and atop by the intra upper Hauterivian reflector (iuH). The BCU appears as a high amplitude reflector. The iuH reflector has a negative amplitude with variable magnitude and continuity. In the shallow Fingerdjupet Subbasin and the Hammerfest Basin, sequence 0 has a subparallel to divergent reflection configuration with good continuity and strong amplitudes (Figs. 3 and 4). The sequence has a wedge-shaped geometry, were there is a distinct thickness increase towards the main depocenters. In the deeper Bjørnøya and Tromsø basins, the reflectors are typically subparallel and discontinuous with low amplitude.

4.1.2. Sequence 1 (Hauterivian – Early Barremian)

Sequence 1 is bounded at the base by the iuH reflector, and atop by the intra Barremian reflector (iB). The iB reflector has a medium negative amplitude with relatively good continuity. The sequence is present in the shallow Hammerfest Basin and Fingerdjupet Subbasin, as well as in the deep Tromsø and Bjørnøya basins, though exhibiting varying thickness and seismic characteristics. In the shallow basins, reflectors are usually parallel to subparallel with strong amplitudes and good continuity. The sequence has a sheet and wedge geometry, where thickness variations are controlled by normal faults. In the Tromsø and Bjørnøya basins, reflectors are subparallel and discontinuous with low amplitude.

4.1.3. Sequence 2 (Barremian – Early Aptian)

Sequence 2 is bounded at the base by the iB reflector and above by the intra lower Aptian reflector (ilA; Fig. 2). Reflectors within sequence 2 are subparallel and continuous with medium amplitude in the Hammerfest Basin. In the Fingerdjupet Subbasin, the sequence is represented by sigmoidal clinoforms with medium to high amplitudes. In the Bjørnøya and Tromsø basins, reflectors have a subparallel to divergent configuration, where wedges are located close to the fault complexes (e.g. LFC, BFC and RLFC). These reflectors have low – medium amplitude and are discontinuous towards the deeper basin segments.

4.1.4. Sequence 3 (Aptian – Early Albian)

Sequence 3 is bounded at the base by the ilA and atop by the intra lower Albian reflector (ilAl). Reflectors within the sequence are subparallel to chaotic and amplitudes are generally low to medium. In places, the sequence has a wedge-shaped geometry, typically thickening towards basin bounding faults, but generally have a sheet-like geometry in the deep basins. No visible negative high-amplitude anomalies have been detected within this sequence.

4.1.5. Sequence 4 (Early Albian – Late Albian)

Sequence 4 is bounded at the base by the ilAl reflector and atop by the intra upper Albian (iuAl) reflector. Reflector configurations range from continuous and parallel to chaotic in the shallow basins, while they are typically subparallel in the deeper basins. The amplitudes are often medium to low. The external geometry of the sequence has sheet to sheet drape external form.

4.1.6. Sequence 5 and 6 (Late Albian – Cenomanian)

Sequence 5 and 6 are grouped together due to similarities in internal seismic characteristics and the internal lack of extensive and significant negative high-amplitude anomalies. Note however, that these sequences are seismically distinguishable from each other as demonstrated by previous workers (e.g. Marín et al., 2017, Figs. 3 and 4). The composite sequence 5 and 6 are bounded at the base by the iuAl reflector and atop by the intra upper Cenomanian reflector (iuCn). The sequences and their corresponding lower and upper bounding surfaces are widespread in the Hammerfest and Tromsø basins and partly in the Bjørnøya Basin but are missing/eroded in the Fingerdjupet Subbasin (Fig. 3). Internally, the reflectors of sequences 5 and 6 are typically parallel to subparallel continuous, with medium amplitude. These sequences generally have a 'basin-infill' geometry, where the greatest thicknesses occur in the deepest parts of the respective basins.

4.2. Potential Lower Cretaceous source rock units

Four negative high-amplitude reflectors have been recognized and mapped in detail within the study area. These are the: i) intra upper Hauterivian (iuH; corresponding to flooding surface K0 of Marín et al., 2017), ii) intra Barremian (iB; corresponding to flooding surface K1 of Marín et al., 2017), iii) intra lower Aptian (ilA; corresponding to

Table 2
Summary of seismic expression and distribution of the negative amplitude reflectors which are coupled to potential source rock units with elevated TOC values, and their typical wireline signal in key wells across the SW Barents Shelf. The wells marked in bold record source rock units with an increased potential.

Reflector	Seismic expression	Occurrence	Key wells	Typical wireline signal GR, DEN, AC, RDEP.	TOC range (average)
Intra upper Hauterivian (iuH)	Continuous, low – medium negative amplitudes	Fingerdjupet Subbasin	7321/7-1	78 gAPI 2.4 g/cm^3 120 us/ft 6.3 Ohm.m	1.48–1.87 wt % (1.68 wt %)
	Continuous, medium – high negative amplitudes	Hammerfest Basin	**7120/8–3** **7120/6-3S** 7120/6-1 **7120/9–2** 7119/9-1 7119/12-1	130–170 gAPI 2.0–2.65 g/cm^3 90–105 us/ft 3–7 Ω m	2.09–5.73 wt % (3.47 wt %)
	Continuous, low negative amplitudes	Bjørnøya Basin	7219/8-1 S	120 gAPI 2.4 g/cm^3 90 us/ft 3.5–5 Ω m	2.58–3.58 wt % (3.17 wt %)
Intra Barremian (iB)	Continuous, low – high negative amplitude characteristics	Hammerfest Basin	**7120/6-3S** **7120/5–1**	115–130 gAPI 2.5–2.6 g/cm^3 90–100 us/ft 3–5 Ω m	1.71–4.88 wt% (3.01 wt %)
	Discontinuous, low negative amplitude characteristics	Bjørnøya Basin	7219/8-1 S	100 gAPI 2.54 g/cm^3 110 us/ft 3–4 Ω m	1.60–2.77 wt % (2.35 wt %)
	Continuous, varying amplitude, low –high negative amplitude characteristics	Fingerdjupet Subbasin	**7321/9–1**	up to 308 gAPI 2.23 g/cm^3 No AC up to 15.7 Ω m	4.00–5.30 wt % (4.50 wt %)
Intra lower Aptian (ilA)	Continuous, medium – high negative amplitude	Hammerfest Basin	**7120/7–3** 7120/6-3 S 7119/9-1	60–85 gAPI 2.3–2.7 g/cm^3 70–100 us/ft 2.5–3 Ω m	0.59–4.56 wt % (2.45 wt %)
	Continuous – discontinuous, low – medium negative amplitude	Bjørnøya Basin	**7219/8-1S**	120–130 gAPI 2.4–2.5 g/cm^3 85–95 us/ft 2.5–4.2 Ω m	3.07–4.42 wt % (3.44 wt %)
Intra upper Cenomanian (iuCn)	Continuous, low – medium negative amplitude	Tromsø Basin	**7218/11–1**	125–140 gAPI 2.2–2.4 g/cm^3 115–130 us/ft 1.9–4.5 Ω m	1.54–3.44 wt % (2.68 wt %)

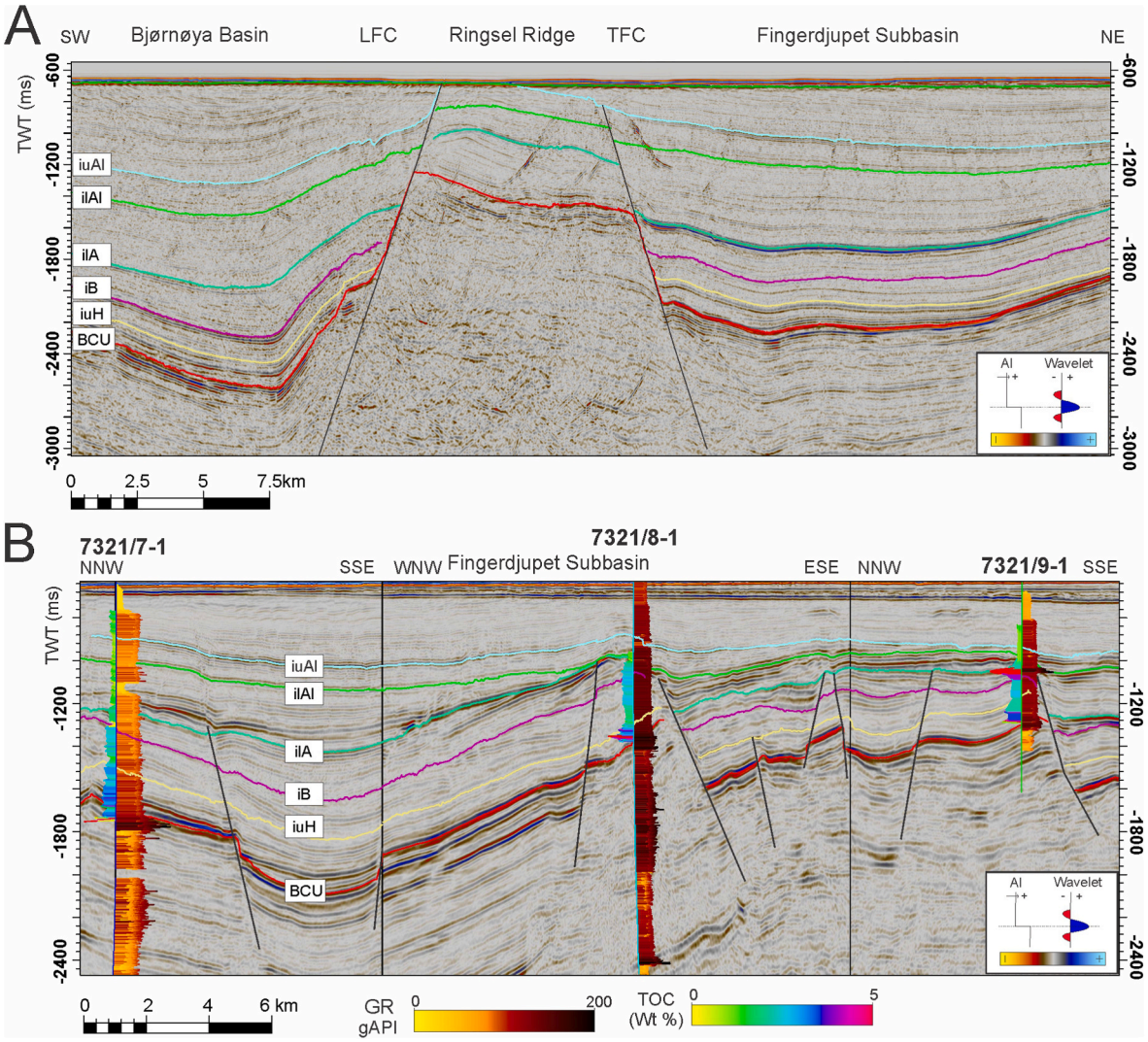

Fig. 5. (A) Seismic section showing the sequence bounding flooding surfaces in the NE part of the Bjørnøya Basin and the main depocenter of the Fingerdjupet Subbasin. Note the prominent negative amplitude associated with the ilA reflector in the Fingerdjupet Subbasin. These basins are separated by the Ringsel Ridge, which is bounded on either side by the Leirdjupet (LFC) and Terningen Fault Complexes (TFC). (B) Composite seismic profile from the Fingerdjupet Subbasin displaying the stratigraphic framework and seismic tie to exploration wells 7321/7–1, 7321/8–1, and 7321/9–1. TOC logs is displayed to the left and GR logs to the right of the individual drill-stems (this is valid for all the following figures). Location of the seismic lines and the wells is shown in Fig. 1. Abbreviations: iuAl: intra upper Albian, ilAl: intra lower Albian, ilA: intra lower Aptian, iB: intra Barremian, iuH: intra upper Hauterivian, BCU: Base Cretaceous Unconformity. Seismic data courtesy TGS and Spectrum.

flooding surface K2 of Marín et al., 2017), and the intra upper Cenomanian (iuCn; corresponding to flooding surface K6 of Marín et al., 2017) reflectors. Each of these reflectors correlate to certain wireline signals in the wells and raised TOC contents, which are typically associated with the presence of organic-rich units. The seismic expression, occurrence, typical wireline signal and TOC range of these units are summarized in Table 2 with a detailed description of each reflector/organic-rich unit given below.

4.2.1. *Intra upper Hauterivian (iuH) reflector*

Fig. 5A shows the stratigraphic framework for the central basin in the Fingerdjupet Subbasin and the transition to the Bjørnøya Basin over the Ringsel Ridge. In addition, a composite seismic profile trough wells 7321/7–1, 7321/8–1 and 7321/9-1 shows the interaction between well, reflector and structural setting in Fig. 5B. The iuH reflector is present across the Fingerdjupet Subbasin and can be traced laterally towards the Bjarmeland Platform (Fig. 5B). The reflector is characterized by continuous low – medium amplitudes, with the strongest amplitudes recorded in the central parts of the basin (see iuH; Fig. 5A). Wells 7321/7–1, 7321/8–1 and 7321/9–1 penetrate the iuH reflector in the Fingerdjupet Subbasin (Fig. 5B). However, the unit corresponding to the reflector has no significant TOC values or wireline signals that would indicate a viable source rock for the area (see iuH; Fig. 6).

The iuH reflector can be traced from the Fingerdjupet Subbasin over the Ringsel Ridge into the Bjørnøya Basin (Fig. 5A). In the Bjørnøya Basin, the iuH reflector has a lower amplitude compared to Fingerdjupet

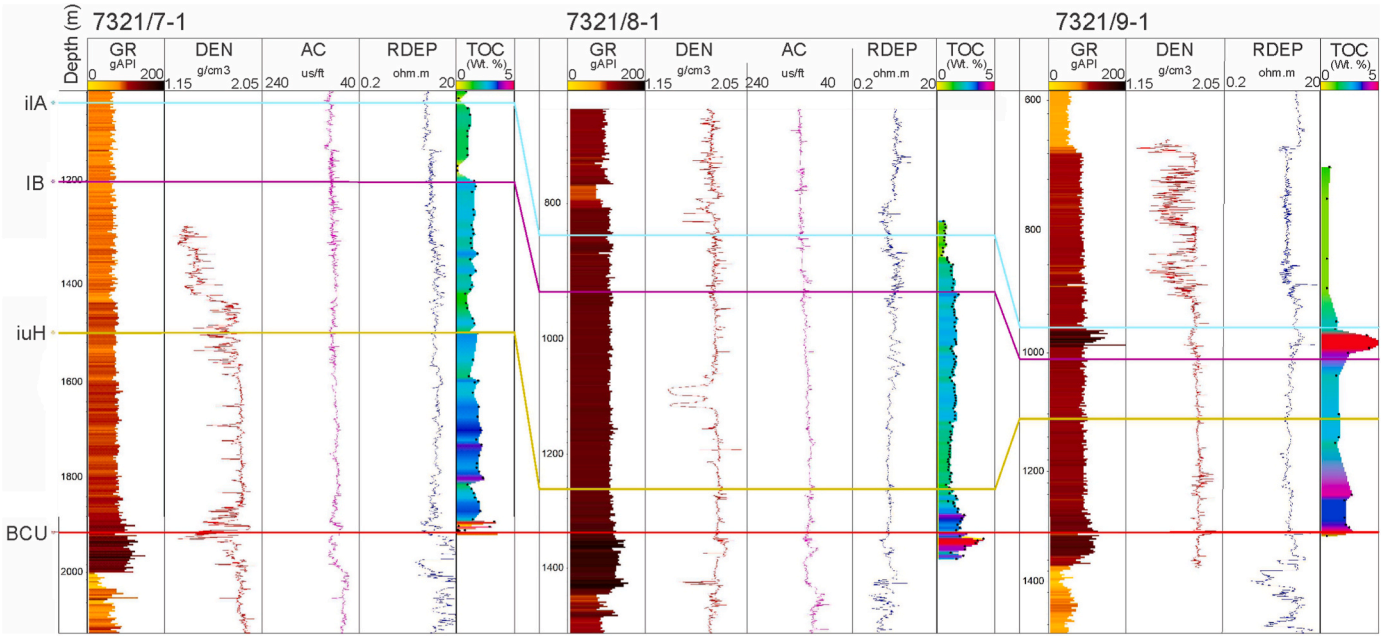

Fig. 6. Correlation of wells 7321/7–1, 7321/8–1 and 7321/9–1 in the Fingerdjupet Subbasin with the BCU (Base Cretaceous Unconformity), iuH (intra upper Hauterivian), iB (intra Barremian), ilA (intra lower Aptian) reflectors annotated. Abbreviations: GR: Gamma ray, DEN: Density, RDEP: Deep Resistivity, TOC: Total organic content. The black circles along the TOC log are sample points. Position of the wells are shown in Fig. 1.

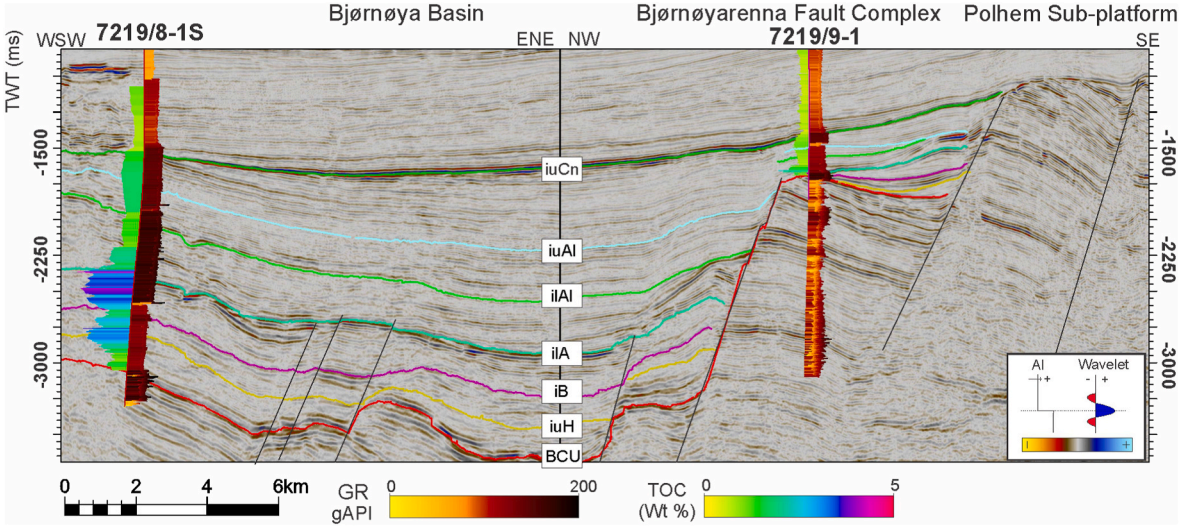

Fig. 7. Seismic composite line displaying the stratigraphic framework in the southern parts of Bjørnøya Basin near the Bjørnøyrenna Fault Complex. The TOC and GR logs is displayed along the left- and right-hand side of the drill-stems, respectively. Note the TOC spikes associated with the iuH and ilA reflectors in the Bjørnøya Basin. Location of the seismic line is indicated in Fig. 1. Abbreviations: iuAl: intra upper Albian, ilAl: intra lower Albian, ilA: intra lower Aptian, iB: intra Barremian, iuH: intra upper Hauterivian, BCU: Base Cretaceous Unconformity. Seismic data courtesy TGS and Spectrum.

Subbasin. However, the reflector remains continuous and can be traced southwards parallel to the BFC. Moving east, towards the deeper parts of the Bjørnøya Basin, the reflector dims to a discontinuous low amplitude reflector. In the southern parts of the Bjørnøya Basin, the iuH reflector is penetrated by well 7219/8-1 S (Fig. 7). Here, the reflector marks the top of a potential source rock unit ranging from 3620 to 3670 m (Figs. 7 and 8). The unit has relatively good TOC content but there is a lack of wireline response to the TOC values (Table 2 and Fig. 8).

In the Hammerfest Basin, the iuH reflector is widely distributed, but onlaps towards the uplifted central high (Fig. 9). The reflector has a medium amplitude with good continuity in the NW corner of the basin but increase in amplitude towards the uplifted central high (see iuH; Fig. 9). In the transition to the Tromsø Basin, the reflector dims but remains continuous until the reflector extends past the RLFC. In wells

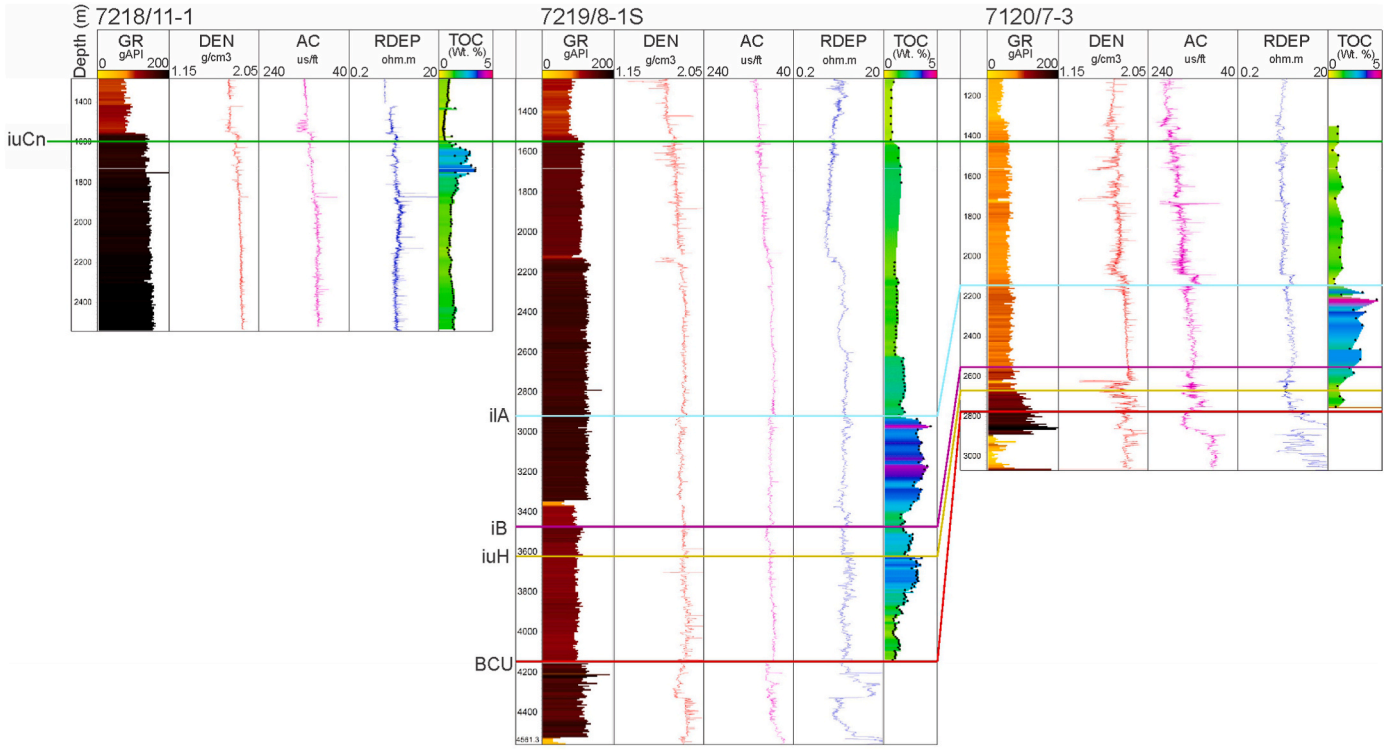

Fig. 8. Correlation panel of wells 7218/11–1, 7219/8-1 S and 7120/7–3 in the Tromsø Basin with the BCU (Base Cretaceous Unconformity), iuH (intra upper Hauterivian), iB (intra Barremian), ilA (intra lower Aptian), and iuCn (intra upper Cenomanian) reflectors annotated. Gamma ray (GR), Density (DEN), deep Resistivity (RDEP) and total organic carbon content (TOC; from Rock-Eval analysis) is included for each well. Note the prominent TOC spike associated with the ilA reflector in well 7120/7-3 located in the faulted transition zone between the Tromsø and Hammerfest Basins. Well location is indicated in Fig. 1.

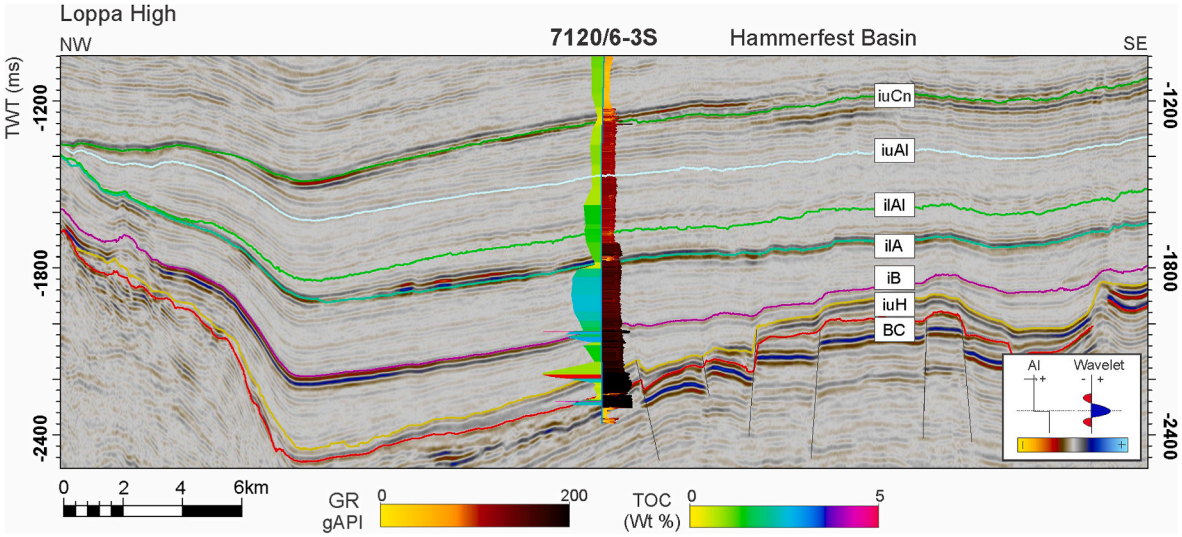

Fig. 9. Seismic section from the Hammerfest Basin showing the NW depocenter and the uplifted central high further to the SE. Here, exploration well 7120/6-3 S is a key well for the Lower Cretaceous succession and record spikes in the TOC-profile associated with the iuH, iB and the ilA reflectors. Abbreviations: iuAl: intra upper Albian, ilAl: intra lower Albian, ilA: intra lower Aptian, iB: intra Barremian, iuH: intra upper Hauterivian, BCU: Base Cretaceous Unconformity. Location of the seismic section is indicated in Fig. 1.

7120/8–3, 7120/6-3 S, and 7119/9–1 the unit corresponding to the iuH reflector have an average thickness of 17 m, and record increased TOC contents (Table 1 and Fig. 10) The wireline logs show a response to the increased TOC values with a drop in DEN values, and increase in both RDEP and AC values (e.g. iuH reflector in well 7120/6-3 S; Fig. 10).

Further towards the west, the iuH reflector is downfaulted along the RLFC into the deeper Tromsø Basin. The reflector quickly loses its seismic characteristics due to deeper burial but can be traced along the NE margin of the Tromsø Basin. At this location, the iuH reflector is discontinuous and characterized by low amplitudes. However, towards the deeper parts of the Tromsø Basin, the reflector is too obscure to be traced with confidence due to the large burial depth and the poorer-quality seismic signal. In addition, there are no well data available from the deep basin.

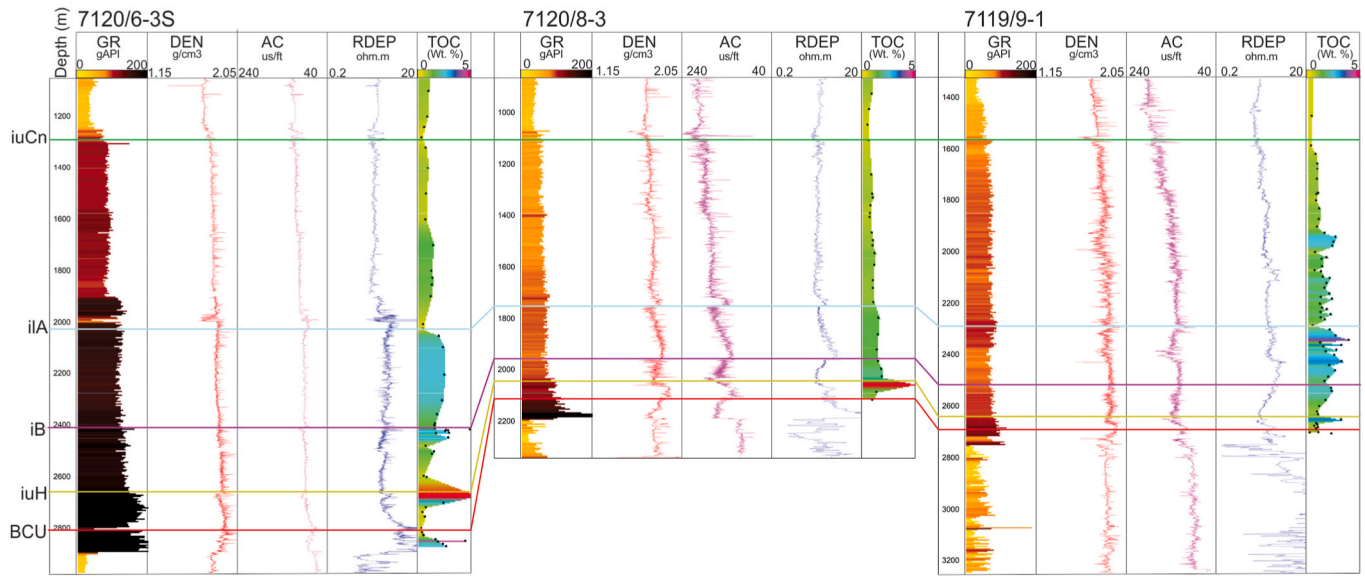

Fig. 10. Well correlation from the Hammerfest Basin including wells 7120/6-3 S, 7120/8–3 and 7119/9–1 with the BCU (Base Cretaceous Unconformity), iuH (intra upper Hauterivian), iB (intra Barremian), ilA (intra lower Aptian), and iuCn (intra upper Cenomanian) reflectors annotated. Prominent TOC spikes is associated with the iuH, iB and ilA reflectors. Well locations are indicated in Fig. 1.

Based on the seismic amplitudes, the wireline signals, and the elevated TOC contents, the iuH reflector is interpreted to represent a potential upper Hauterivian source rock unit in the Hammerfest Basin. The iuH reflector thus marks the top of this unit in well 7120/8–3, 7120/6-3 S, 7119/9–1 and 7120/9–2, which have a clear GR-log trend with associated high TOC values (Fig. 10). Data from well 7120/6-3 S record high TOC values close to the Loppa High and the AFC. However, at this location the amplitude is lower than on the central high. In addition, well 7120/8–3, 7119/9–1 and 7120/9–2 indicate that the organic-rich unit may hold potential in the central parts of the basin. This could indicate that the organic-rich unit is more widely distributed in the Hammerfest Basin, not only occurring in localized depocenters near the Loppa High and the Finnmark Platform.

Despite a small increase in TOC in well 7321/7–1, the low amplitude of the reflector coupled with the unfavorable wireline signals and the generally low TOC values, indicate that there is no potential associated with iuH reflector in the Fingerdjupet Subbasin. In the Bjørnøya Basin, the iuH reflector has a low – medium amplitude associated with the unit in well 7219/8-1 S. This 50 m thick unit has relatively high TOC values. However, the low RDEP values show little to no response to possible liquid petroleum in the unit.

4.2.2. Intra Barremian (iB) reflector

The iB reflector is extending across the entire Fingerdjupet Subbasin as a continuous, but low amplitude negative reflector (Fig. 5A). The reflector is penetrated by three wells in the Fingerdjupet Subbasin and may be correlated to a unit which record a relatively small increase in TOC contents (Fig. 5B; Table 2). However, the TOC levels are relatively low and wireline logs indicate there is no significant response to the slightly increased TOC values (see iB reflector; Fig. 6). From the Fingerdjupet Subbasin, the iB reflector can be traced to the Bjørnøya Basin over the Ringsel Ridge (Fig. 5A) and further south, parallel along the LFC and BFC. The reflector is generally discontinuous and characterized by a low amplitude close to these fault complexes. Towards the deeper parts of the Bjørnøya Basin, the reflector dims significantly and becomes difficult to interpret. The iB reflector intersects well 7218/8-1 S in the southern parts of the Bjørnøya Basin, where the reflector marks the top of an up to 250 m thick unit with elevated GR and moderate TOC values (Table 2 and Fig. 8).

The iB reflector is distributed over the entire western margin of the Hammerfest Basin. The reflector is continuous, has low – high amplitude characteristics, and interacts with all the wells in the area. However, the reflector has its strongest amplitudes in the NW corner of the Hammerfest Basin, and the reflector dims towards the uplifted central high (Fig. 9). Hence, the nearby wells 7120/6-3 S and 7120/5–1 are regarded as key wells for the iB reflector (Table 2). Furthermore, in well 7120/6-3 S the reflector marks the top of a 48 m tick unit, where the highest TOC values are in the uppermost section of the unit (Table 2; Figs. 9 and 10). Laterally, the TOC content in this unit decrease, demonstrated by well 7120/8-3 situated on the central high and well 7119/9-1 located towards the Tromsø Basin (Fig. 10). At the western transition towards the Tromsø Basin, the reflector is downfaulted along the RLFC and becomes impossible to trace in the deeper basin segments. However, the reflector is traced close to the RLFC in the NE parts of the Tromsø Basin. At this location, the reflector is discontinuous and has a low amplitude. There are no wells in the Tromsø Basin that may provide age-control or wireline data.

Based on the wireline logs, TOC values and amplitude characteristics the iB reflector may represent a potential intra Barremian source rock unit in the NW part of the Hammerfest Basin (i.e. wells 7120/6-3 S and 7120/5–1). The negative amplitude of the reflector increases in magnitude towards the Loppa High and the AFC, this might indicate an increased potential. Laterally, the extensive reflector is penetrated by all the wells on the western margin of the Hammerfest Basin, but the TOC contents and wireline values measured in the corresponding unit do not indicate widespread potential. In the Fingerdjupet Subbasin, the iB reflector is of low amplitude and the TOC content is low in wells 7321/7–1, 7321/8–1 and 7321/9–1. In addition, there is no response in the RDEP or GR log. Hence, there is no evidence for an intra Barremian source rock unit in the Fingerdjupet Subbasin. In the adjacent Bjørnøya Basin, the iB reflector marks the top of a unit exhibiting increased GR values in well 7219/8-1 S. However, there are no increases in the TOC values nor do the wireline logs indicate that there is any source rock potential.

4.2.3. Intra lower Aptian (ilA) reflector

The ilA reflector is widespread in the Fingerdjupet Subbasin but is eroded on the local highs (i.e. well 7312/8–1; Fig. 5B). Amplitude characteristics varies laterally, but the reflector has a distinct negative amplitude in the central basin and the southern parts of the Fingerdjupet

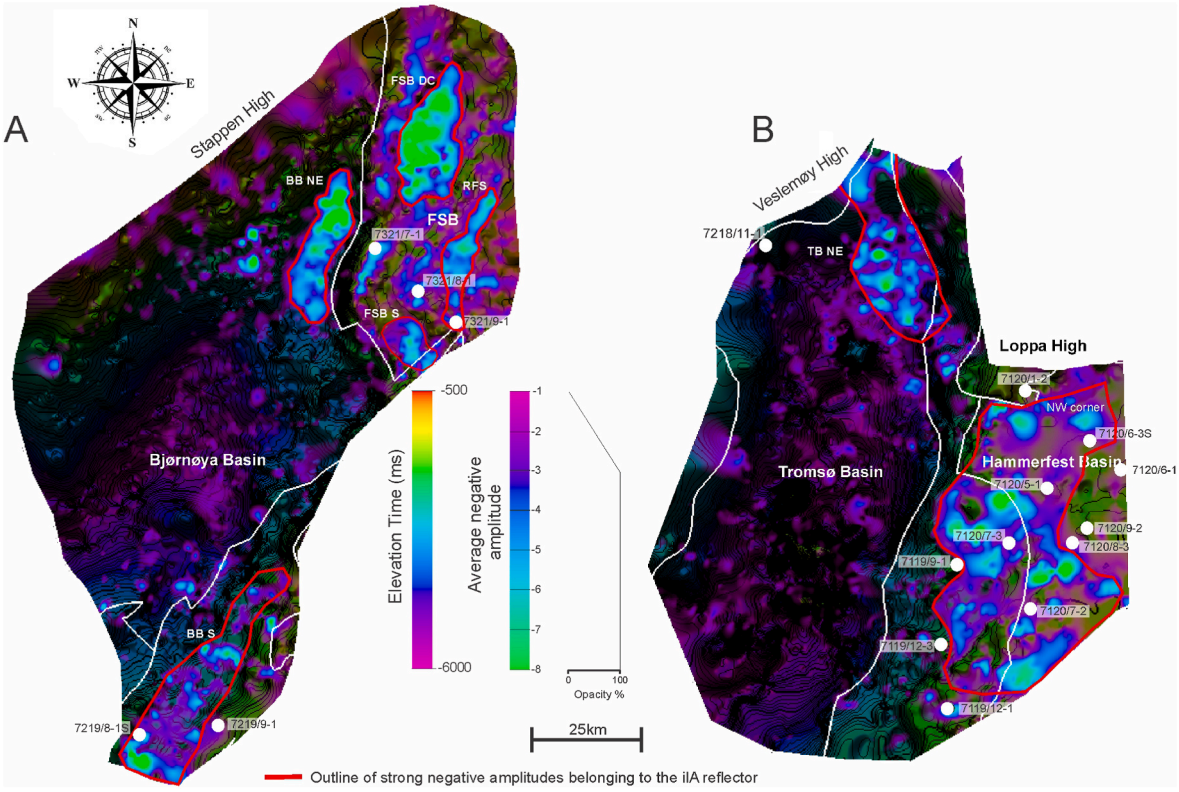

Fig. 11. A) Average negative amplitude and elevation map of the ilA reflector in the Fingerdjupet Subbasin and the Bjørnøya Basin. The negative amplitude map is overlying the elevation map with gradual opacity, in order to highlight the strongest negative amplitudes. B) Average negative amplitude and elevation map of the ilA reflector in the Hammerfest and Tromsø Basins. Outline of structural elements based on maps available at NPD Factpages (2021). Abbreviations: BB: Bjørnøya Basin, FSB; Fingerdjupet Subbasin, RFS: Randi Fault Set, TB: Tromsø Basin, DC: depocenter.

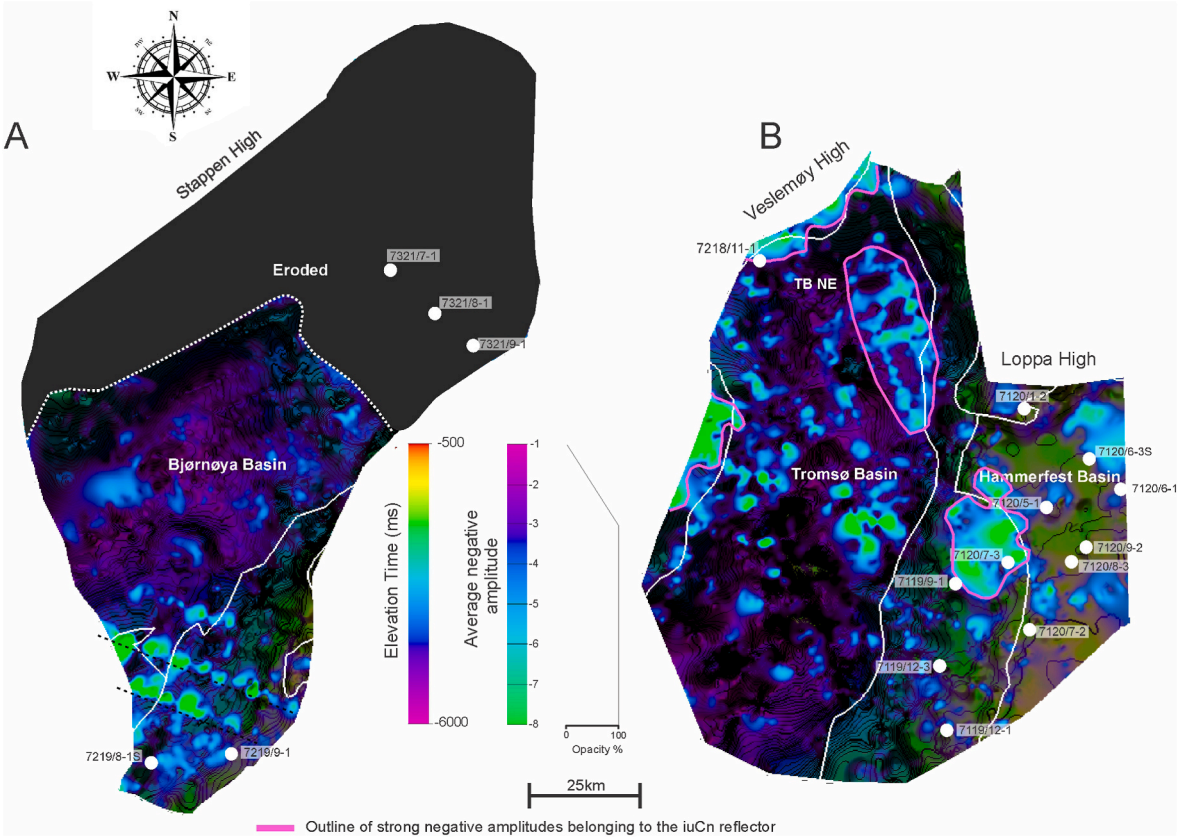

Fig. 12. A) Average negative amplitude and elevation map of the iuCn reflector in the Bjørnøya Basin. The negative amplitude map is overlying the elevation map with gradual opacity, in order to highlight the strongest negative amplitudes. B) Average negative amplitude and elevation map of the iuCn reflector in the Tromsø and Hammerfest Basins. Outline of structural elements based on maps available at NPD Factpages (2021).

Subbasin (Fig. 5A). These negative high amplitudes are illustrated in the negative amplitude map, which show the lateral extent and magnitude of the negative ilA reflector in the Fingerdjupet Subbasin and the Bjørnøya Basin (Fig. 11A). Smaller bright-spots are also sporadically present north of well 7321/9–1 and towards the eastern margin of the Fingerdjupet Subbasin (Fig. 11A). Distribution of these high amplitudes are delimited by local highs controlled by the TFC, LFC and RFS (Figs. 5A–11A).

The ilA reflector is eroded in well 7321/8-1 but it intersects wells 7321/7–1 and 7321/9–1 (Fig. 5B). In well 7321/7–1, there is little indication of a potential source rock unit as the c. 50 m thick unit have low TOC and GR values (Fig. 6). In addition, the RDEP and AC logs do not display any elevated values (Fig. 6). In well 7321/9–1, the ilA reflector marks the top of a 24 m thick unit (levels 961–985 m; Fig. 6), which internally contains five sections of high GR-values and elevated TOC contents (Fig. 6) In addition, the DEN values drop and there is a significant increase in RDEP values (Table 2 and Fig. 6).

The ilA reflector is also mapped in the Bjørnøya Basin. The strongest negative amplitudes are in the NE part of the basin, dimming southwards (Fig. 11A). However, it is still possible to trace it parallel to the LFC and BFC towards well 7219/8-1 S, where the reflector has good continuity and a medium amplitude (Fig. 11A). The reflector is also extending laterally towards the deeper parts of the Bjørnøya Basin, where the reflector dims into a low amplitude reflector of poor continuity (Fig. 11A). Well 7218/8-1 S penetrates the ilA reflector and a 159 m thick unit (Table 1). The unit has a clear increase in TOC values and wireline logs show a small response to the increased TOC values (Table 2 and Fig. 8).

The ilA reflector has a basin-wide distribution in the Hammerfest Basin and typically has a medium to high amplitude with good continuity (Figs. 9–11B). High amplitude patches are sporadically distributed, with some confined to NW part close to the AFC (Fig. 11B). These high amplitude patches are located some distance away from key wells such as 7120/6-3 S and 7119/9–1 (Fig. 11B) but interact with others (e.g. 7120/7–3).

The ilA reflector marks the top of increased TOC values in multiple wells in the Hammerfest Basin (e.g. 7120/6-3 S, 7120/7–3 and 7119/9–1; Figs. 9 and 10). The thickness of these units varies between each

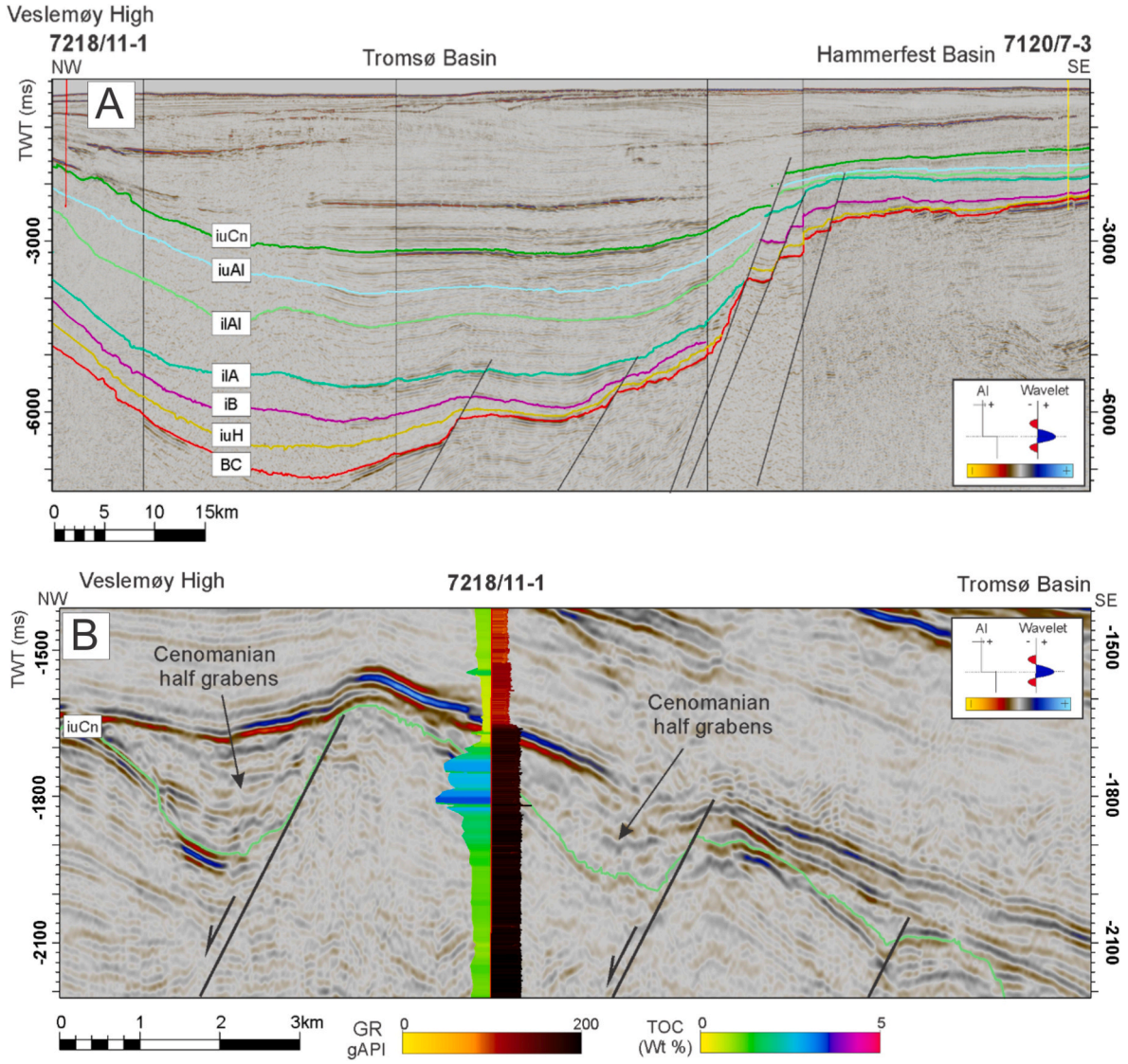

Fig. 13. (A) Seismic composite line covering the NE part of the Tromsø Basin and the western margin of the Hammerfest Basin. Exploration well 7218/11–1 is located in the northern parts of Tromsø Basin and is a key well for the iuCn reflectors which is associated to an inferred upper Cenomanian source rock unit. (B) Seismic section zoomed-in on well 7218/11–1. Here, the iuCn reflector can be traced to the Tromsø Basin across a series of small fault-bound half-graben basins. The TOC-profile shows a pronounced response associated with this reflector. Abbreviations: iuAl: intra upper Albian, ilAl: intra lower Albian, ilA: intra lower Aptian, iB: intra Barremian, iuH: intra upper Hauterivian, BCU: Base Cretaceous Unconformity. Location of the seismic section is indicated in Fig. 1.

Table 3
TOC and Rock-Eval characteristics of the four interpreted source rock units with the highest potential. Average values have been used for each sample interval (Table 1). HI: Hydrogen index, OI: Oxygen index.

Potential source rock unit	Well	Location	TOC wt. %	S2 mg HC/g rock	HI mg HC/g TOC	OI mg CO_2/g TOC	T_{max} °C	Kerogen Type	Vitrinite reflectance (R_o)	Maturity
upper Hauterivian	7120/8-3	Western margin of the Hammerfest Basin	5.02	3.3	67	7	440	III	0.81	Peak mature
	7120/6-3 S		4.07	5.16	130	17	453	II	N/A	Late mature
	7120/9-2		2.09	5.6	265	N/A	N/A	III	N/A	N/A
Barremian	7120/6-3 S	Western margin of the Hammerfest Basin	2.92	8.42	279	11	440	II	N/A	Early mature
	7120/5-1		3.29	3.8	115	11	442	III	0.81	Peak mature
lower Aptian	7321/9-1	Fingerdjupet Subbasin	4.50	19.4	428	11	436	II	N/A	Early mature
	7120/7-3	Western margin of the Hammerfest Basin	3.0	2.9	87	21	446	II-III	0.68	Peak mature
	7219/8-1 S	Southern parts of Bjørnøya Basin,	3.44	3.4	107	63	450	III	0.89	Late mature
upper Cenomanian	7218/11-1	Northern edge of the Tromsø Basin	2.68	7.03	259	35	427	II–III	0.30	Immature

well (Table 1) and common for these units is the lack of wireline response to the elevated TOC values (Table 2). When traced laterally across the RLFC, the ilA reflector changes into a low amplitude reflector with poor continuity, which persists across major parts of the Tromsø Basin. (Fig. 11B). The reflector has medium amplitudes with good continuity in the NE part of the basin (Fig. 11B). Here, the reflector is located at depth of c. 5500 ms, implying that any organic matter has most likely reached very high maturity. In addition, there are no wells in the Tromsø Basin that penetrate the ilA reflector to confirm its potential.

Based on wireline logs, increased TOC values and amplitude characteristics, the ilA reflector is interpreted to represent a potential source rock unit in the Fingerdjupet Subbasin. The potential may extend from well 7321/9–1 towards the deeper parts of the basin in the southern and central parts of the Fingerdjupet Subbasin. In addition, bright spots recorded within the RFS north of well 7321/9–1 may indicate some potential. The reflector also shows favorable amplitude characteristics in the NE part of the Bjørnøya Basin, in proximity to the LFC and the Ringsel Ridge.

Indication of a viable source rock unit is also documented in the Hammerfest Basin. Although there are several wells recording elevated TOC contents, there are no other favorable indications in the wireline data (e.g. well 7120/6-3 S, 7120/7–3 and 7119/9–1). However, the negative amplitude map suggests sporadically distributed bright spots that may indicate an increased potential in the NW part of the basin (i.e., near the AFC). In the NE margin of the Tromsø Basin, the ilA reflector has increased amplitude compared to in the rest of the basin. However, it is positioned at a depth of c. 5500 ms, which implies that any organic matter most likely has reached very high maturity.

4.2.4. *Intra upper Cenomanian (iuCn) reflector*

The iuCn reflector is only present in the deeper parts of the Bjørnøya Basin as it is eroded in the Fingerdjupet Subbasin and across the Stappen High. (Fig. 12A). The iuCn reflector is continuous with low – medium amplitudes, which increases to medium – high further south in the basin towards well 7219/8-1 S (Figs. 7–12A). Elongated high amplitude anomalies are also present in this area (Fig. 12A). The reflector terminates against the BFC on the western margin of the Loppa High but extends across the Veslemøy High to the west of well 7219/8-1 S (Fig. 12A). In well 7219/8-1 S, the corresponding 43 m thick unit records a small increase in TOC values (Table 2). However, the wireline logs indicate that there is no significant response to the TOC content (Fig. 8).

The iuCn reflector is present along the entire western segment of the Hammerfest Basin, delimited by the Loppa High and the Finnmark Platform (Fig. 12B). The reflector is continuous and has a medium – high amplitude, where local high amplitudes occur along the western margin of the basin and towards the Loppa High (Fig. 12B). High amplitude patches are located around key wells such as well 7120/6-3 S near the Loppa High, and well 7120/7–3 towards the Tromsø Basin (Fig. 12B). The iuCn reflector is penetrated by all the wells in the western Hammerfest Basin, but common for these wells is that there is no indication of elevated TOC values associated with this event.

The iuCn reflector is traced from the Hammerfest basin across the RLFC into the Tromsø Basin (Fig. 13A). Here, the amplitude characteristics changes to a lower amplitude, but remains continuous. The reflector extends laterally throughout the basin and the negative amplitude map shows that strong negative amplitudes are present in the central parts and along the basin edges (Fig. 12B). NNE – SSW-oriented, elongated amplitude anomalies are also present across the basin (Fig. 12B).

Well 7218/11–1 is one of few wells that penetrates the iuCn reflector in the Tromsø Basin (Fig. 13A and B). From the seismic data, it is clear that this well is positioned in a half-graben setting near the basin margin (Fig. 13B). At this location, the iuCn reflector has a low – medium amplitude (Fig. 13B). The corresponding 121 m thick unit in the well has elevated TOC values, but wireline logs indicate that there is little to no response to the increased organic matter beneath the iuCn reflector (Table 2 and Fig. 8).

Although the iuCn reflector is penetrated by key wells in the Bjørnøya, Hammerfest and Tromsø basins, there are no TOC values or wireline signals that convincingly demonstrate the presence of a potential upper Cenomanian source rock unit. However, there are some elevated TOC values in well 7218/11–1. The general lack of response in the wireline logs may indicate that the concentration of organic matter is too low to produce a signal characteristic for prolific source rock units.

4.3. *Source rock evaluation of the organic-rich units*

Based on the mapping of the four high-amplitude negative reflectors in the seismic data (i.e. the iuH, IB, ilA, and iuCn reflectors; Table 2) combined with analyses of the wireline and TOC data, four organic-rich units representing potential source rock units are suggested. These includes: 1) upper Hauterivian, 2) Barremian, 3) lower Aptian, and 4) upper Cenomanian units. These potential source rock units occur atop of sequences 0, 1, 2 and 6, respectively (Fig. 2). Source rock characteristics based on the available Rock-Eval data (see Table 1 for sample interval, and the online supplementary file SF1 for the raw data) are given for each of these potential source rock units. The main characteristics of the

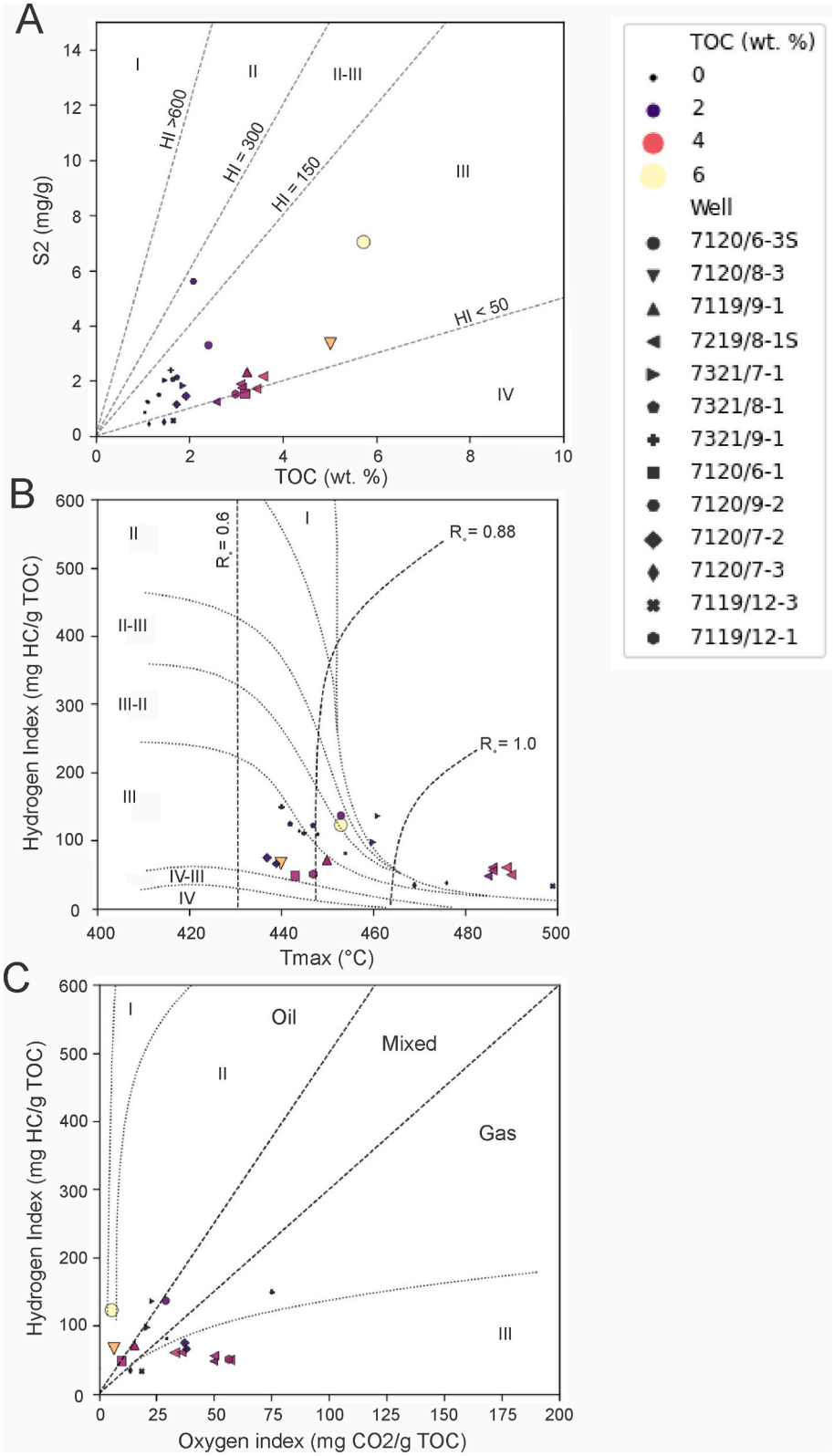

Fig. 14. Plots showing the potential of the Hauterivian source rock unit (corresponding to the iuH reflector) in key wells across the SW Barents Shelf. Sample points increase in size depending on TOC values. Sample points from each well have a specific marker. Location of the wells are shown in Fig. 1. The sample interval and thickness are shown in Table 1 (A) Cross-plot of TOC vs. Rock-Eval S2 values, overlying are the hydrogen index (HI) lines which indicate kerogen type. (B) Plot of T_{max} vs. HI indicating the petroleum potential and maturity of the samples. Overlying are the vitrinite reflectance (Ro) lines after Isaksen and Ledje (2001). (C) van Krevelen diagram of HI vs. OI indicating the quality and maturation level of the samples.

units with highest potential are summarized in Table 3.

4.3.1. Characteristics of the upper Hauterivian organic-rich unit

The characteristics of the upper Hauterivian organic-rich unit is shown in Fig. 14. In general, most of the analyzed samples have poor potential indicated by low S2 values (S2 < 2.5 mg/g) and variable TOC content (1.0–5.7 wt %; Fig. 14A). They also have low HI (50–150 mg HC/g TOC; Fig. 14B) and OI values (1–75 CO_2/g TOC; Fig. 14C). Furthermore, the same samples appear to be mature with T_{max} values of 430–460 °C (Fig. 14B) and near the vitrinite reflectance trend line 0.88%

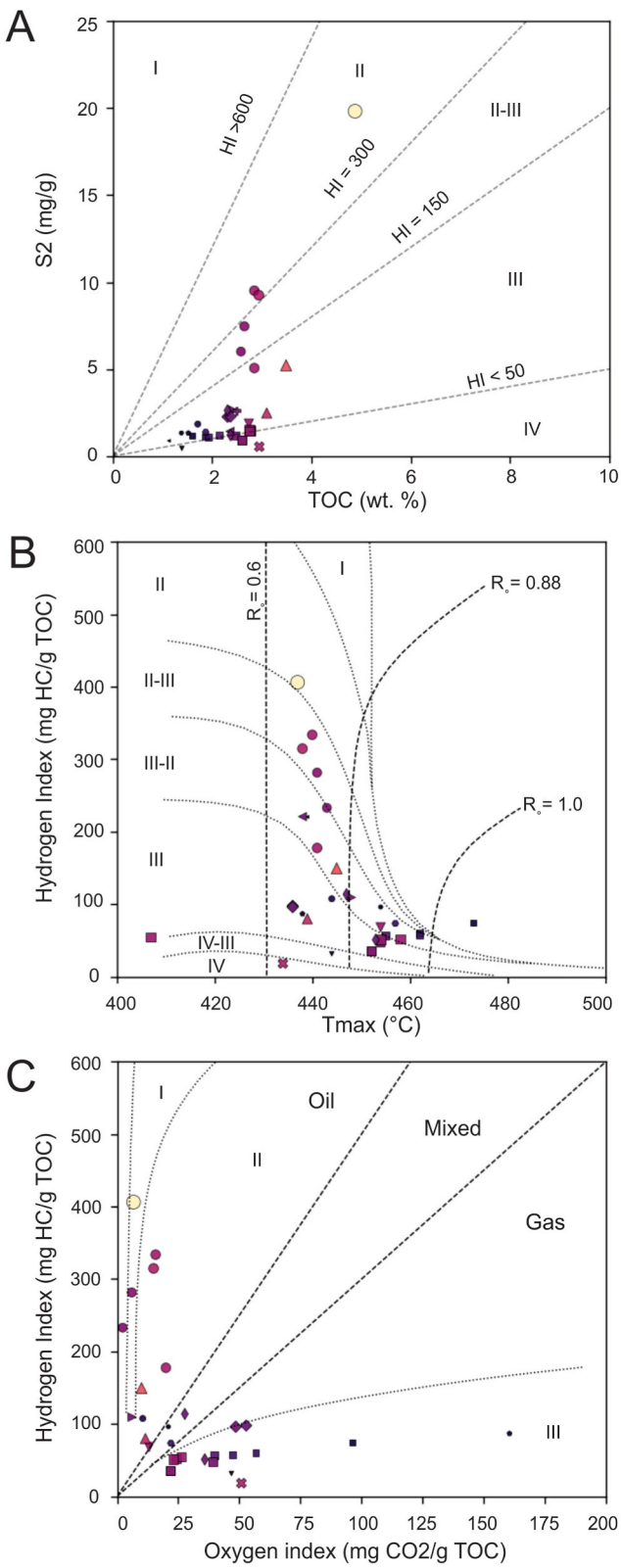

Fig. 15. Plots showing the potential of the Barremian source rock unit (corresponding to the iB reflector) in key wells across the SW Barents Shelf. Sample points increase in size depending on TOC values. Sample points from each well have a specific marker. Location of the wells are shown in Fig. 1. The source rock units thickness and data is shown in Table 1 (A) Cross-plot of TOC vs. Rock-Eval S2 values, overlying are the hydrogen index (HI) lines which are indicating kerogen type. (B) Plot of T_{max} vs. HI indicating the petroleum potential and maturity of the samples. Overlying are the vitrinite reflectance (Ro) lines after Isaksen and Ledje (2001). (C) van Krevelen diagram of HI vs. oxygen index (OI) indicating the quality and maturation level of the samples.

(Fig. 14B). Collectively, the majority of the samples indicate that kerogen Type III dominates the upper Hauterivian organic-rich unit and that gas is the main expelled product (Fig. 14C).

A few sample points deviate from the general trend of the organic-rich unit and may reflect more localized potential. This includes samples from wells 7120/8–3, 7120/6-3 S and 7120/9–2, which all show higher potential (Table 3 and Fig. 14A). However, these units are relatively thin and contain few sample points (Table 1). Well 7120/6-3 S contains the most prolific sample of the Hauterivian organic-rich unit. These samples have higher HI values and plots within the kerogen Type II field (Fig. 14C). No vitrinite reflectance data is available for well 7120/6-3 S.

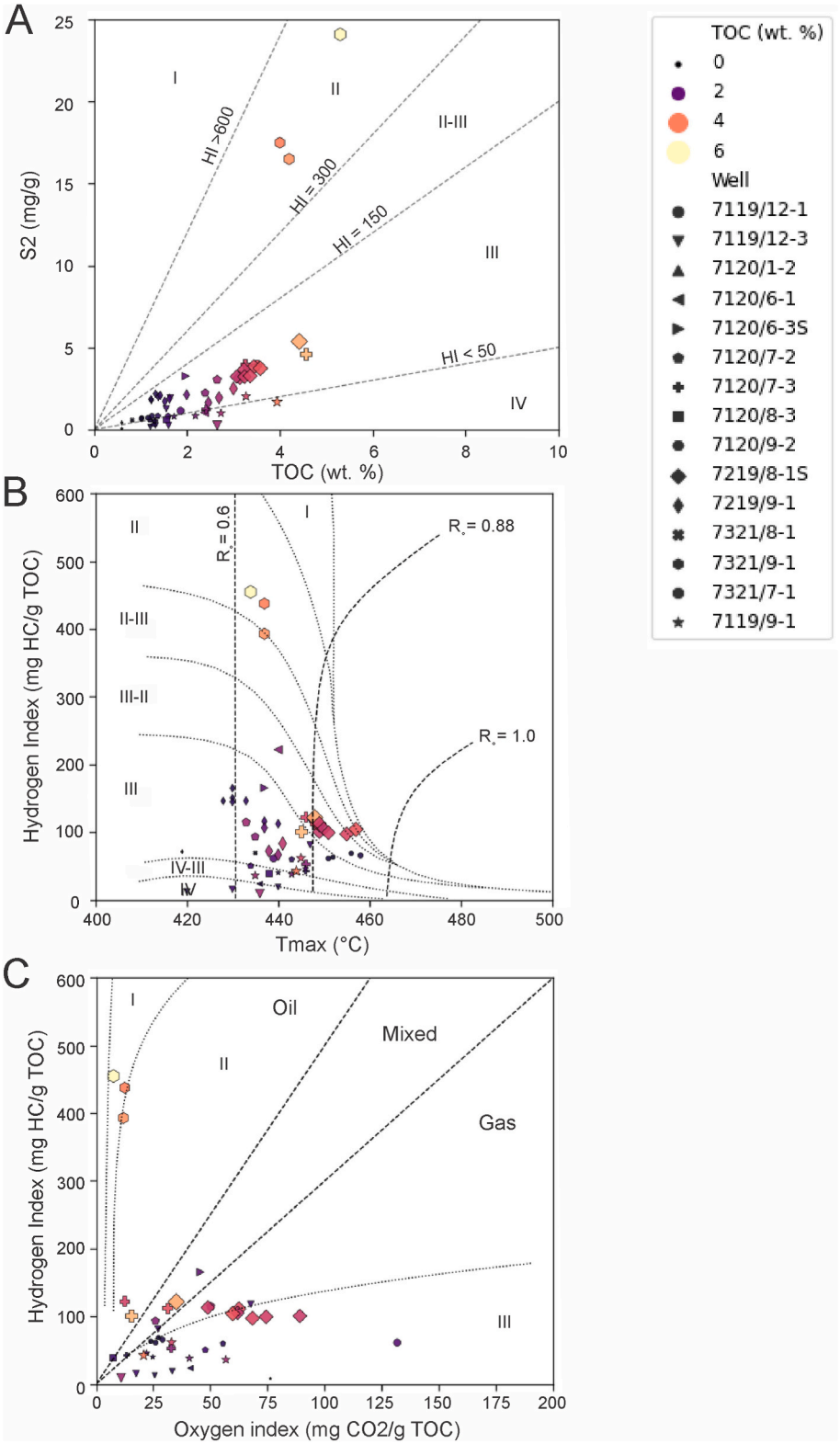

Fig. 16. Plots showing the source rock potential of the Lower Aptian source rock unit (corresponding to the ilA reflector) in key wells across the SW Barents Shelf. Sample points increase in size depending on TOC values. Sample points from each well have a specific marker. Location of the wells are shown in Fig. 1. The source rock thickness and data is shown in Table 1 (A) Cross-plot of TOC vs. Rock-Eval S2 values, overlying are the hydrogen index (HI) lines which are indicating kerogen type. (B) Plot of T_{max} vs. HI indicating the petroleum potential and maturity of the samples. Overlying are the vitrinite reflectance (Ro) lines after Isaksen and Ledje (2001). (C) van Krevelen diagram of HI vs. OI indicating the quality and maturation level of the samples.

4.3.2. *Characteristics of the Barremian organic-rich unit*

Fig. 15 shows the source rock evaluation of the samples from the Barremian organic-rich unit. The general trend shows that most of the samples have a poor potential indicated by low S2 values (S2 < 2.5 mg/g) and a variable TOC content (1.13–4.88 wt %; Fig. 15A). In addition, most of the samples have low HI values (50–150 mg HC/g TOC) and T_{max} values of 430–470 °C (Fig. 15B). The samples also have low OI values (1–100 CO_2/g TOC; Fig. 15C). In total, most of the data indicate a mature (Fig. 15B) kerogen Type III dominated (Fig. 15C) organic-rich unit, with poor potential (Fig. 15A).

The source potential of the Barremian organic-rich unit seems to be very localized demonstrated by samples in wells 7120/6-3 S and 7120/5–1, as these stand out as the most prolific ones (Table 3 and Fig. 15A). The most prolific sample is taken from well 7120/6-3 S and has a S2

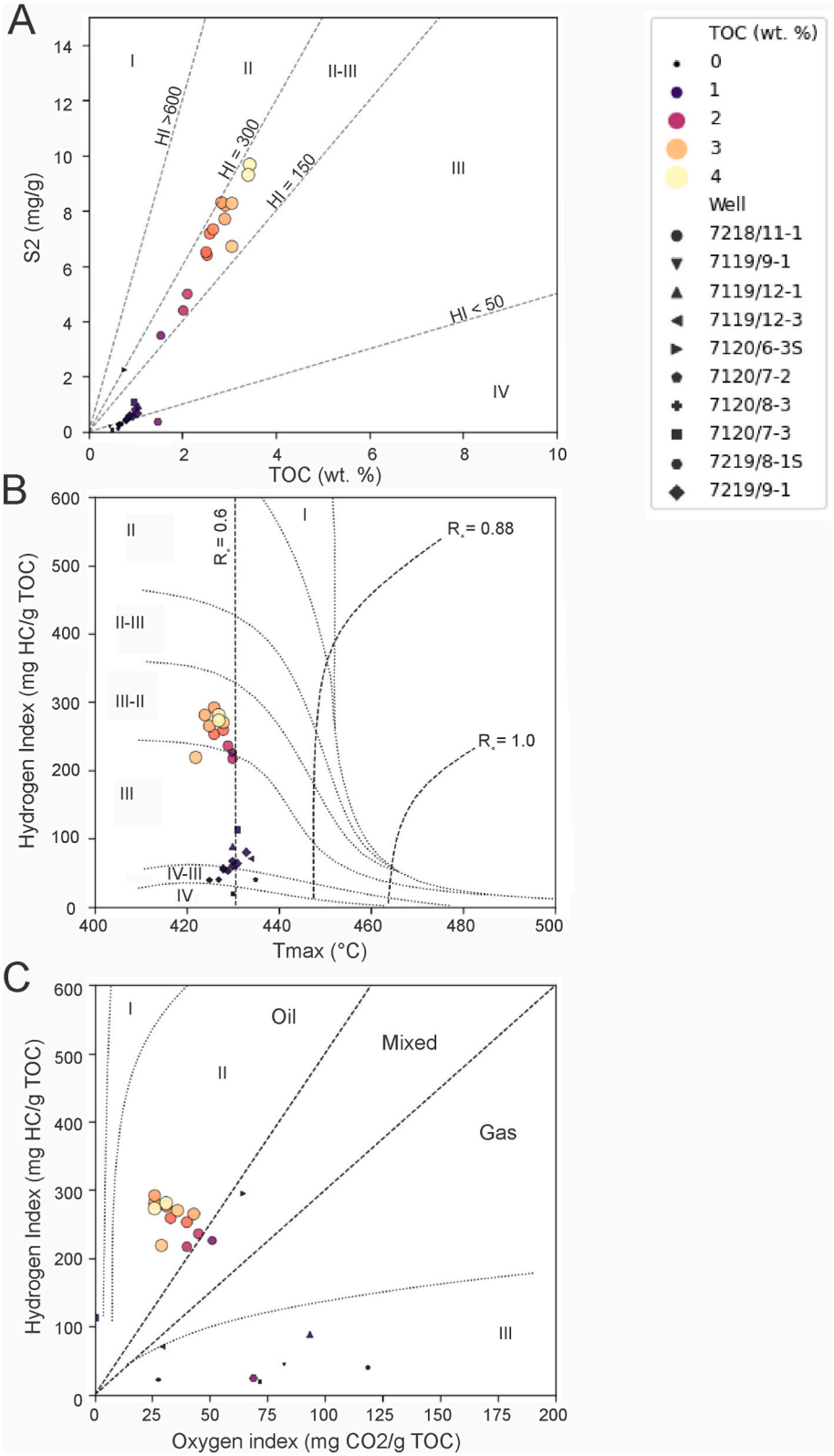

Fig. 17. Plots showing the source rock potential of the Cenomanian source rock unit (iuCn) in key wells across the SW Barents Shelf. Sample points increase in size depending on TOC values. Sample points from each well have a specific marker. Location of the wells are shown in Fig. 1. The source rock units thickness and data is shown in Table 1 (A) Cross-plot of TOC vs. Rock-Eval S2 values, overlying are the hydrogen index (HI) lines which are indicating kerogen type. (B) Plot of T_{max} vs. HI indicating the petroleum potential and maturity of the samples. Overlying are the vitrinite reflectance (Ro) lines after Isaksen and Ledje (2001). (C) van Krevelen diagram of HI vs. OI indicating the quality and maturation level of the samples.

value of 19.82 mg/g and TOC values of 4.88 wt% (Fig. 15A). In general, samples in well 7120/6-3 S exhibit higher hydrogen content (Table 3 and Fig. 15B). In addition, T_{max} values are on average 440 °C, while the vitrinite reflectance (R_o) ranges between 0.6 and 0.88% (Fig. 15B). Collectively, the Barremian organic-rich unit in well 7120/6-3 S has excellent potential with a kerogen Type II composition and is further classified as an early mature to mature oil prone source rock unit.

4.3.3. *Characteristics of the lower Aptian organic-rich unit*

The source rock evaluation on the samples from the lower Aptian organic-rich unit is shown in Fig. 16. Most of the samples are plotting in the poor potential area with low S2 values (S2 < 2.5 mg/g) and

generally low TOC content (1.5–3 wt %; Fig. 16A). These samples have HI values close to 100 mg HC/g TOC and are plotting around T_{max} values of 440 °C to the right of the $R_o = 0.6$ vitrinite reflectance trend line (Fig. 16B). The same cluster also has variable OI values (1–100 CO_2/g TOC) coupled with low HI values (Fig. 16C). Collectively, this indicate that most of the lower Aptian organic-rich samples have a kerogen Type III composition where the expected product would be gas.

A few samples from wells 7321/9–1, 7219/8-1 S, and 7120/7-3 deviate from the general trend and indicate a localized higher potential (Table 3 and Fig. 16A). The most prolific samples for the lower Aptian organic-rich unit are from well 7321/9–1 and have a kerogen Type II composition (Table 3; Fig. 16A and B) No vitrinite reflectance data are available for this source rock unit but based on T_{max} values and the vitrinite reflectance $R_o = 0.6$ trend line, the organic-rich unit is early mature (Fig. 16B). The organic-rich unit has also low OI values and high HI values, implying that the organic-rich unit is high quality and that the main expelled product is oil (Fig. 16C).

Multiple samples from the organic-rich unit in well 7219/8-1 S and 7120/7–3 also indicate elevated potential (Table 3). However, this unit has significantly lower HI values compared to well 7321/9–1 and has a kerogen Type III composition (Fig. 16A and B). The exceptional high T_{max} values in well 7219/8-1 S plot to the right of the $R_o = 0.88\%$ vitrinite reflectance trend line, indicating that the organic-rich unit is mature at this locality (Fig. 16B). Furthermore, based on the OI and HI values the main expelled product is gas from the organic-rich unit in well 7219/8-1 S (Fig. 16C). In contrast, the samples in well 7120/7-3 plots to the left of the $R_o = 0.88$ vitrinite reflectance trend line (Fig. 16B) and within the oil window (Fig. 16C).

4.3.4. Characteristics of the upper Cenomanian organic-rich unit

The source rock evaluation performed on the samples from the upper Cenomanian organic-rich unit is displayed in Fig. 17. Apart from samples in well 7218/11–1, most of the samples show a unimodal distribution with very poor potential, indicated by low S2 (S2 < 2.5 mg/g) and TOC values (0.83–1.49 wt %; Fig. 17A). These samples also have low HI values (20–110 mg HC/g TOC) and variable T_{max} values (422–435 °C; Fig. 17B). This indicates that the small amount of organic matter is most likely of kerogen Type IV–III composition (Fig. 17A and B) and that the main product is gas (Fig. 17C).

The exception is well 7218/11–1 which overall shows a better potential with substantially higher TOC and S2 values (Table 3 and Fig. 17A). Samples from 7218/11–1 also have higher HI values and slightly lower T_{max} values compared to the low potential samples (Table 3 and Fig. 17B). Hence, these samples plot left of the vitrinite reflectance trend line $R_o = 0.6$ (Fig. 17B). In addition, three samples of vitrinite reflectance are available for the unit. These samples have little spread and have an average R_o value of 0.3%. In total, this classifies the organic matter in well 7218/11–1 as a kerogen Type II-III (Fig. 17C) where the main expelled product is oil (Fig. 17C). However, based on the T_{max} values and the vitrinite reflectance samples, the organic-rich unit is classified as immature at the well location.

5. Discussion

The presence of four organic-rich units of variable source rock potential has been documented within the Lower Cretaceous succession on the SW Barents Shelf, these are the: (1) upper Hauterivian (2) Barremian, (3) lower Aptian, and (4) upper Cenomanian organic-rich units (Table 3). These units have different characteristics which result in varying potential across the region. This may reflect variations in depositional environments and oxygen levels, organic productivity, and preservation potential governed by amongst other factors such as sedimentation rate, basin configurations and hydrodynamic conditions.

During the Early Cretaceous, active rifting in the SW Barents Sea resulted in a typical rift configuration with fault-bounded basins separated by structural highs (e.g. Faleide et al., 1984, 1993a, b; Marin et al., 2018a, b). At times when the structural highs were submerged, well-oxygenated hydraulic regimes may have persisted across the highs, whereas stagnant, oxygen deficient conditions may have prevailed in the deeper parts of the basins due to physical restriction and reduced bottom water circulation (e.g. Langrock et al., 2003). Consequently, wells targeting the structural highs that formed during the Early Cretaceous structuring-events, typically sample Lower Cretaceous stratigraphy which most likely exhibit low quantity and quality organic matter. Thus, elevated TOC and HI values, as well as increased source potential are generally expected for the deeper parts of the Early Cretaceous fault-bounded depocenters (e.g. Karlsen et al., 2004: Karlsen and Skeie, 2006). In addition, the data only give an indication of the remaining potential at the prevailing levels of thermal maturity. At early burial, the organic matter was less mature and had higher quality and quantity. Understanding variations in depositional environments and burial history of the potential source rock units is therefore essential. Below, a depositional model for each of the organic-rich units are presented, emphasizing various factors controlling their source potential, particularly focusing on the areas where they have been confirmed by exploration wells and thus hold the greatest potential.

5.1. Controls on source rock distribution and potential

To form a viable source rock unit there must be sufficient primary biological productivity in the depositional environment (Calvert et al., 1996). Primary productivity near continental margins in the marine environment is dependent on nutrient influx either by fluvial run-off or upwelling of deep marine water (Demaison et al., 1983). The Loppa High which is situated in the center of the study area, was subaerially exposed during the Early Cretaceous (Faleide et al., 1993a; Indrevær et al., 2017) and was most likely a crucial source for influx of both sediments and nutrients (e.g. Seldal, 2005; Marín et al., 2017, 2018a; Ärlebrand et al., 2021). In addition, the warm and humid climate characterizing the Cretaceous period, promoted increased organic productivity and biotic changes (Leckie et al., 2002; Scotese et al., 2021) that was crucial for organic matter to be deposited (e.g. Rogov et al., 2020).

Furthermore, the formation of fault bounded depocenters on the SW Barents Shelf and further south along the western margin of the NCS during the Late Jurassic – Early Cretaceous (e.g. Langrock et al., 2003), resulted in restricted circulation and anoxic conditions that ensured optimal preservation conditions, further prohibiting oxidative processes, degradation and consumption of organic matter (Demaison and Moore, 1980). These anoxic to suboxic conditions are also regarded as being the product of climatic variations associated with oceanic anoxic events (OAEs) (Leckie et al., 2002; Midtkandal et al., 2016; Rogov et al., 2020). However, the variations and differences in richness and quality of the organic matter is strongly linked to regional and local paleogeographic factors that affected the basin infill history.

Other controlling factors include grain size and sedimentation rate. Grain size has implications towards preservation of organic matter, as coarse-grained sediments may allow circulation of oxygenated bottom waters into the sediments (Bordovskiy, 1965). In the study area, this could be a localized issue near active sediment source areas such as the Loppa High but for the wider SW Barents Shelf, most of the Cretaceous sediments appear to consist of marine mudrocks with low permeability. Sedimentation rate has a crucial control on the concentration of organic matter, as high rates will cause a dilution effect (Ibach, 1982). According to literature, sedimentation rate should ideally be approximately 1 mm/year (Ibach, 1982; Bohacs et al., 2005). This could be problematic for potential source rock units situated in the Bjørnøya and Tromsø basins, as the Late Jurassic – Early Cretaceous rifting phase caused rapid subsidence and increased sedimentation rates along the RLFC and BFC (Faleide et al., 1984, 1993a, 1993b; Kairanov et al., 2021). In addition, the arrival of large prograding delta systems in the Barremian to early Aptian (from the NW) and in the Albian to Cenomanian (from the E to

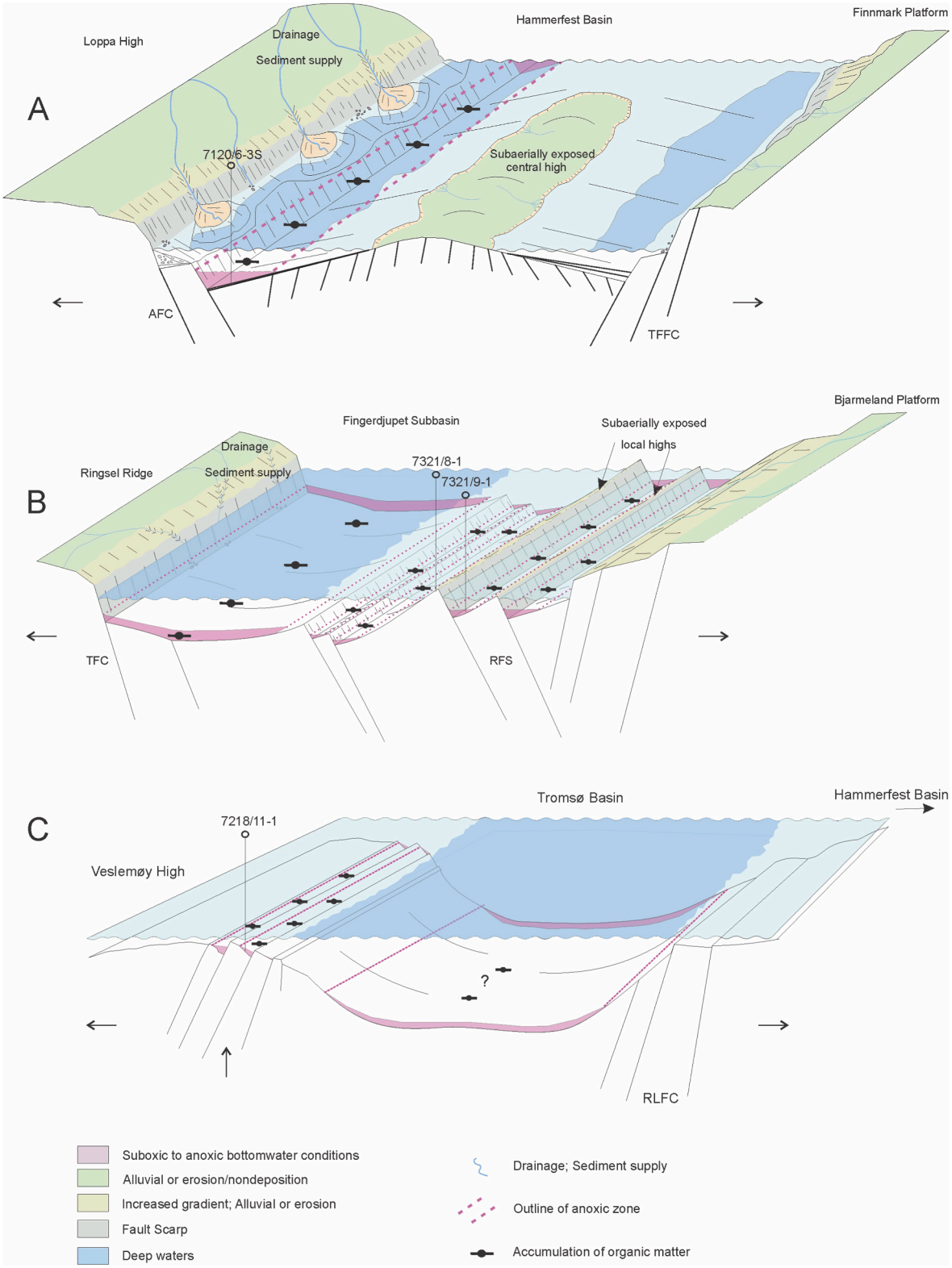

Fig. 18. (A) Depositional model outlining the basin configuration and conditions during deposition of (A) the Hauterivian and Barremian source rock unit in the Hammerfest Basin, (B) the lower Aptian source rock unit in the Fingerdjupet Subbasin, and (C) the upper Cenomanian source rock unit at the transition to the Veslemøy High. Abbreviations: AFC: Asterias Fault Complex, TFFC: Troms Finnmark Fault Complex, RLFC: Ringvassøy Loppa Fault Complex, LFC: Leirdjupet Fault Complex, RFS: Randi Fault Set.

NE) may locally have contributed to increased sedimentation rates and consequently lowered the source rock potential in the receiving basins during these times.

5.1.1. Depositional model and source rock potential of the upper Hauterivian organic-rich unit

The evaluation of the Hauterivian organic-rich unit shows that most of the samples have a kerogen Type III composition with variable TOC content and low S2 values (S2 < 2.5 mg/g). This includes the wells in the Fingerdjupet Subbasin (7321/7–1.7321/8–1, 7321/9–1) and the southern parts of Bjørnøya Basin (7219/8-1 S). The unit was established as mature to overmature in the shallow basins and essentially overmature in well 7219/8-1 S (Fig. 14A). Based on the maturity data in well 7219/8-1 S (Fig. 16) and the lateral mapping of the iuH reflector, we interpret that there is presently no source rock potential for the Hauterivian organic-rich unit in the deep basins, caused by deep burial and compaction. However, a few wells in the Hammerfest Basin (7120/8–3, 7120/6-3 S, 7120/9–2) have higher potential indicated by higher S2 and HI values (Fig. 14A and B). The most prolific samples are taken from well 7120/6-3 S, located close to the NW part of the Hammerfest Basin (Figs. 9 and 10).

The upper Hauterivian organic-rich unit is also present in a more condensed form towards the central high of Hammerfest Basin (e.g. wells 7120/8–3 and 7120/9–2, Fig. 14). The iuH reflector extends further towards the transition to Tromsø Basin. In this transition, the reflector is part of the down-stepping array of normal faults of the RLFC. Source rock evaluation done on samples from wells located in this transition (e.g. 7120/7–2, 7120/7–3, 7119/9–1, 7119/12–3 and 7119/12–1) confirms that the iuH reflector is not associated with a high potential source rock unit (Fig. 14). This supports our interpretation of a localized prolific upper Hauterivian organic-rich unit confined to a restricted depocenter, such as the NW part/segment of the Hammerfest Basin.

According to Ohm et al. (2008) the Knurr Formation (which includes the Hauterivian organic-rich unit of this study; Fig. 2) has a higher potential than the Kolje and Kolmule formations. Their study was predominantly focused on the Hammerfest Basin, where most exploration wells in the SW Barents Sea are located. Their initial findings suggest a low potential for the Knurr Formation, which is in accordance with our source rock evaluation (Fig. 14). However, we emphasize that there is an increased potential in the shallow depocenter of Hammerfest Basin (i.e. in well 7120/6-3 S, NW part). Still, very few exploration wells have drilled the thick sedimentary successions in these depocenters, as most exploration wells typically target structural highs.

The SW Barents Shelf was subject to multiple episodes of rifting during the Late Jurassic – Early Cretaceous extensional event (Faleide et al., 1984, 1993a, 1993b; Gabrielsen et al., 1990; Serck et al., 2017; Kairanov et al., 2021). The elevated potential documented in the NW part of the Hammerfest Basin is clearly linked to the patchy occurrence of smaller fault-bound depocenters that formed during the earliest Cretaceous. It is well known that structural confinement of marine basins may result in restricted water circulation, which eventually lead to oxygen deficient conditions that promote the preservation of organic matter (Demaison and Moore, 1980; Demaison et al., 1983).

We thus envisage that the upper Hauterivian organic-rich unit in the Hammerfest Basin was deposited and preserved in a partly restricted marine setting, between the subaerially exposed Loppa High and the uplifted central arch (Figs. 10–18A). This depocenter formed in response to faulting along the AFC, which was initiated in the Late Jurassic – earliest Cretaceous (Wood et al., 1989; Gabrielsen et al., 1990). The uplifted central arch acted as intrabasinal highs where onlap terminations in sequence S0 and S1 indicate periodic subaerial exposure (Fig. 10) (Indrevær et al., 2017; Marín et al., 2018b). To the north, the Loppa High was subaerially exposed at these times (Faleide et al., 1993a, 1993b) due to periodic and differential uplift that shifted the drainage patterns and promoted the development of incised valleys that routed sediments to the basin (Fig. 18A) (Indrevær et al., 2017; Marín et al., 2018b). In this configuration, the NW corner of the Hammerfest Basin was a partly restricted, bounded between two subaerially exposed structural highs (Marín et al., 2018b). Consequently, this gave the characteristic wedge shape of sequence S0 and S1 in the NW corner but also resulted in increased preservation potential for organic matter. (Fig. 18A). Deep-water conditions prevailed in the central parts of the Hammerfest Basin which was connected to the Tromsø Basin in the west securing better water circulation (Fig. 18A; Marín et al., 2018b).

The kerogen Type III composition characterizing the upper Hauterivian organic-rich unit, suggest that most of the organic matter is of terrestrial origin or of a partly oxidized type possibly including a resedimented fraction (Tissot et al., 1973; Peters, 1986; Peters and Cassa, 1994). The nearby subarial exposed Loppa High was most likely a source for the organic matter, which was transported to the basin by gravitational processes (Fig. 18A). In contrast, the source rock unit in well 7120/6-3 S has a more dominant kerogen Type II composition (Fig. 14C). This may indicate that organic matter accumulated under restricted water circulation which allowed suboxic to anoxic conditions to develop (Demaison and Moore, 1980; Demaison et al., 1983). The nearby sediment source area also ensured high nutrient influx into the marine environment, allowing high productivity under the warm and humid climatic conditions that prevailed during the earliest Cretaceous (Fig. 18A).

5.1.2. Depositional model and source rock potential of the Barremian organic-rich unit

The iB reflector is widely distributed on the SW Barents Shelf and is penetrated by wells in the Fingerdjupet Subbasin, the Bjørnøya Basin and the Hammerfest Basin. Despite its wide distribution, most samples belonging to the Barremian organic-rich unit indicate a mature unit with a kerogen Type III composition yielding low generation potential (Fig. 15; Tables 2 and 3). Similar to the upper Hauterivian organic-rich unit, the most prolific unit occurs in well 7120/6-3 S and 7120/5–1 at the NW corner of the Hammerfest Basin (Fig. 15 and Table 3). At this location, the Barremian organic-rich unit have a kerogen Type II composition (Fig. 15C).

In the Fingerdjupet Subbasin, the iB reflector is located on top a SE-prograding sequence which probably was sourced from the Svalbard Platform that experienced significant uplift in the Barremian (Grundvåg et al., 2017; Marín et al., 2017; Midtkandal et al., 2019). In many prolific basins elsewhere, an elevated source rock potential (i.e. kerogen Type II–I) is commonly reported within the top-set to bottomset of similar large-scale prograding clinoform successions (Barker, 1982; Kosters et al., 2000; Ulmishek, 2003). However, based on the mapping of the iB reflector and the lack of response in the wireline and Rock-Eval data (i.e. 7321/7–1, 7321/8–1 and 7321/9–1), we conclude that the Barremian organic-rich unit does not have any potential in the Fingerdjupet Subbasin.

The source rock evaluation conducted on samples belonging to the Barremian organic-rich unit in well 7219/8-1 S indicate that organic matter is of kerogen Type III and do not hold any potential based on low S2 and HI values (Fig. 15A and B). In addition, the unit is classified as post-mature based on T_{max} values and two vitrinite reflectance samples (Fig. 15A). This has wider implication towards the Bjørnøya and Tromsø basins, as any organic matter that belong to the potential Barremian organic-rich unit is most likely post-mature in the deeper basinal segments.

During deposition of the Barremian organic-rich unit, the NW part of the Hammerfest Basin continued to be an important fault-bound depocenter, and the central arch and the Loppa High were still uplifted, both acting as source areas and exhibiting first-order controls on the basin configuration which was essential for anoxic conditions to be maintained (Fig. 18A).

The long-lived restricted character of the NW depocenter of the Hammerfest Basin governed water circulation and promoted water

stratification and anoxic bottom water conditions (Fig. 18A). Increased fluvial run-off (from the Loppa High) and increased primary productivity influenced by the warm and humid climate and an associated oxygen consumption in the water mass further promoted anoxic bottom water conditions (Fig. 18A). This interpretation is coherent with the kerogen Type II composition of the Barremian organic-rich unit in well 7120/6-3 S (Fig. 15).

5.1.3. Depositional model and source rock potential of the lower Aptian organic-rich unit

The seismic mapping and source rock evaluation of the lower Aptian organic-rich unit indicate that there is an elevated potential in the Fingerdjupet Subbasin and possibly also in the Bjørnøya and Hammerfest basins (Table 3). The unit in well 7321/9–1 was established to be the most prolific and is linked to negative amplitudes occurring in localized fault bounded depocenters in the Fingerdjupet Subbasin (Fig. 11A).

The negative amplitudes concentrated around well 7321/9–1 also extends laterally towards the NNE (Fig. 11A) and appear to be confined to half-grabens (Fig. 5B) that most likely link up with the NNE – SSW-oriented RFS (Fig. 11A), cf. Serck et al. (2017). However, the strongest negative amplitudes are confined to the main depocenter of the Fingerdjupet Subbasin (Fig. 11A, controlled by the N–S and NNE – SSW trending faults belonging the TFC and RFS (Serck et al., 2017). Strong negative amplitudes are also present in the southern part of the Fingerdjupet Subbasin (Fig. 11A). These amplitudes occur in a downfaulted section close to the LFC associated with a distinct thickness increase of the sequence S3 strata. This may indicate a connection to the suggested reactivation event in the early Aptian (Serck et al., 2017).

In the Bjørnøya Basin, the lower Aptian organic-rich unit has kerogen Type III composition and is late mature in well 7219/8-1 S (Table 3). The dim negative amplitudes surrounding well 7219/8-1 S (Fig. 11A) further indicate that this area does not hold any high concentration of organic matter. However, based on the lateral mapping, the unit is most likely extending from well 7219/8-1 S parallel to the nearby fault complexes (i.e. BFC and LFC) and could possibly be associated with the strong negative amplitudes present in the NE corner of the basin (Fig. 11A). It thus appears that the lower Aptian organic-rich unit preferably accumulated along the NE basin margins where conditions were favorable. The amount of TOC in marine sediments is controlled by the abundance and availability of organic matter, preservation and the degree of dilution by sedimentary input (Pedersen and Calvert, 1990). It thus seems that the lower Aptian organic-rich unit was subjected to less dilution effect further north towards the LFC. This may relate to a less active local source area of limited extent (i.e. Ringsel Ridge), possibly coupled with delimited or structurally diverted drainage patterns along the major fault complexes in the area. Consequently, this limited sediment input and the dilution effect in this area. In well 7219/8-1 S, the elevated TOC values of the lower Aptian organic-rich unit are confined to a thick interval (159 m; Tables 1 and 2), possibly indicating that depositional conditions were favorable in places, but were generally negatively affected by high sedimentation rates.

The source rock evaluation and the seismic mapping indicate that the lower Aptian organic-rich unit has less potential in the Hammerfest Basin (Fig. 16). The elevated hydrogen content in wells 7120/6–1 and 7120/6-3 S is coupled to relatively low S2 and TOC values (Fig. 16), indicating a limited potential in the NW part of the basin. Well 7120/7–3 is located in the middle of a cluster of high negative amplitudes. Here, the lower Aptian organic-rich unit is demonstrated to be one of the most prolific intervals of the whole succession (Table 3), indicating that there were favorable conditions for organic matter to accumulate and be preserved in the faulted transition to the Tromsø Basin. These conditions seem to be very localized as no other wells located in this transitional zone contain the lower Aptian organic-rich unit (e.g., wells 7119/12–1, 7119/12–3 and 7119/9–1). This points to organic matter accumulation in depocenters along the RLFC.

The structural development of the Fingerdjupet Subbasin with multiple phases of faulting have clearly governed deposition and preservation of the lower Aptian organic-rich unit. The basin development is attributed to reactivation of the N– S- and NNE– SSW-oriented fault complexes (i.e. LFC, TFC and RFS), which follows the trend of older structural lineaments (Serck et al., 2017). These fault complexes were active during the latest Jurassic – Hauterivian and later reactivated in the early Aptian (Serck et al., 2017).

Considering this development and the distribution of the lower Aptian organic-rich unit, we suggest that it accumulated in restricted shallow, half-graben basins associated with movements along the TFC and RFS (Fig. 18B). The rates of subsidence increased during the latest Jurassic – Hauterivian rifting, eventually creating increased bathymetric relief, and promoting the development of syn-tectonic growth wedges near the TFC and RFS (Serck et al., 2017) (Fig. 5A). The subsequent arrival of the SE-prograding clinoform succession (sequence S2, Marín et al., 2017b) during the Barremian filled much of this relief, but was most likely delimited by uplifted footwall highs (Serck et al., 2017) (e.g. location of well 7321/8–1; Fig. 5B). Fault reactivation during the early Aptian renewed the creation of accommodation space in the half-grabens. Coupled with the eustatic sea-level rise and ocean anoxia in the early Aptian (e.g. Schlanger and Jenkyns, 1976; Jenkyns, 1980), this created an ideal setting which allowed organic matter to be preserved in a localized, structurally restricted marine basin (Fig. 18B). The negative amplitude map supports this interpretation, as the greatest negative amplitudes are observed in the half-grabens along the TFC and RFS (Fig. 11A). In addition, the kerogen Type II composition indicates that the organic-rich unit were deposited in a marine environment under anoxic conditions (Demaison and Moore, 1980; Demaison et al., 1983).

Furthermore, the OAE1a has been recorded on the Svalbard Platform (Midtkandal et al., 2016) and linked to a time-equivalent regional extensive lower Aptian flooding surface (Grundvåg et al., 2019). Here, a lower Aptian source rock unit associated with the flooding surface is located atop of a thick coal-bearing paralic succession, testifying to its proximal position near the northern margin of the Barents Shelf at these times. This unit apparently has a localized wet gas potential (e.g. Grundvåg et al., 2019). Although representing deposition under principle different structural settings (i.e. platform versus half graben), the source rock unit on the Svalbard Platform may represent a lateral equivalent to the unit documented in well 7321/9–1 (e.g. Grundvåg et al., 2019) testifying to the high productivity in this period. However, to confidently establish a link between the lower Aptian source rock unit in the Fingerdjupet Subbasin and the OAE1a, carbon and oxygen isotope methodologies should be implemented in the future (e.g. Herrle et al., 2015; Midtkandal et al., 2016; Vickers et al., 2016). There is also the issue of age uncertainties in well 7321/9–1 (Corseri et al., 2018). However, the time-equivalent deposition of the kerogen Type II-III source rock unit on the Svalbard Platform may indicate that the lower Aptian source rock potential is of regional significance, but dependent on structural confinement to generate an oil-prone source rock unit (Grundvåg et al., 2019).

5.1.4. Depositional model and source rock potential of the upper Cenomanian organic-rich unit

Based on the lateral mapping and evaluation of the upper Cenomanian organic-rich unit, we suggest that this unit has greatest potential in the northern part of Tromsø Basin at the transition to the Veslemøy High (Figs. 13B–17). At this location, well 7218/11–1 penetrated an immature unit with a kerogen Type II–III composition (Table 3). This suggests that the upper Cenomanian unit could have source rock potential in similar restricted settings. In addition, the strong negative amplitudes located in the transition to Veslemøy High and the Senja Ridge could indicate that the upper Cenomanian organic-rich unit has increased potential in relation to these highs (Fig. 12B). The elongated amplitudes seen in the amplitude map (Fig. 12) seem to follow the orientation of the seismic lines and could indicate amplitude differences between the surveys.

One central question is whether this potential can be correlated to the negative amplitudes seen in the Tromsø Basin (Figs. 12B and 13A). The restricted character of the depositional setting of the mudrocks sampled in well 7218/11-1 makes such correlation difficult for a wider basin perspective. In addition, exploration wells drilled on local highs and in association with salt domes do not provide the stratigraphic information needed (i.e. 7219/8-1 S, 7119/9–1, 7119/12–3). The Cenomanian source rock potential is, therefore, still unknown in the Tromsø Basin. This is coupled to the likelihood that the basin was well oxygenated and subject to high sedimentation rates associated with the arrival of the delta system prograding from the E and NE during the late Albian and Cenomanian (i.e. sequences 5 and 6; Marín et al., 2017, Fig. 2).

In the Hammerfest Basin, strong negative amplitudes occur in the proximity of well 7120/7–3, possibly indicating abundant organic matter in this area (Fig. 12B). However, the source rock evaluation conducted on samples from well 7120/7-3 shows that there is no Cenomanian source rock potential here (Fig. 17A). Towards the NW corner of the Hammerfest Basin, well 7120/6-3 S records elevated hydrogen content in the upper Cenomanian unit (Fig. 17C). However, the source rock evaluation shows that the unit has low TOC and S2 values, which limit the potential.

The upper Cenomanian organic-rich unit was deposited in a half-graben situated on the northern edge of the Tromsø Basin, as part of the Veslemøy High (Fig. 18C). The development of this half-graben is attributed to the formation a series of NE–SW-striking faults, possibly belonging to the BFC and RLFC (Kairanov et al., 2021). In this area, Valanginian – late Barremian and Aptian – Albian faulting have been documented (Faleide et al., 1993a; Kairanov et al., 2021). This faulting eventually led to rotation of fault blocks and the formation of localized half-graben basins (Fig. 18C). During the Cenomanian, the Veslemøy High was subject to uplift (Kairanov et al., 2021), further restricting the half-graben basins and limiting oxygenated water circulation. This is supported by the kerogen Type II-III composition of the organic-rich unit, which indicates that anoxic to suboxic conditions must have prevailed during deposition (cf. Demaison and Moore, 1980; Demaison et al., 1983).

5.2. Implications for exploration

Exploration well 7219/8-1 S provides an important stratigraphic control for all the Lower Cretaceous organic-rich units in the deep Tromsø and Bjørnøya basins and adjacent areas (Fig. 2). The source rock evaluation conducted on samples from the four potential source rock units investigated in this study, provides an indication as to the potential in the deeper basinal segments.

Data from well 7219/8-1 S establish the lower Aptian unit to be kerogen Type III dominated and in the late mature stages, still part of the oil window. Hence, we conclude that any organic matter deposited before the early Aptian is most likely post-mature in the deeper basinal areas along the RLFC and BFC. This has implications for hydrocarbon exploration in these frontier areas along the western shelf margin. However, the lower Aptian organic-rich unit is considered to have the greatest potential and should consequently be considered when exploration strategies are discussed for the SW Barents Shelf. The presence of a mature to late mature lower Aptian source rock unit in well 7219/8-1 S, may thus represent a local source for exploration targets in the areas surrounding the RLFC and BFC, as well as towards the flanks of the deep basins (Fig. 11A). Because the traditional Upper Jurassic source rock unit is overmature in these areas (Dore, 1995; Marín et al., 2020), the lower Aptian source rock unit could present a viable alternative. However, as there is limited well control in the deep basins, seismic attributes and lateral mapping is key to understanding the distribution and potential of any source rock units distributed along the fault complexes.

We also demonstrate that the lower Aptian unit in well 7219/8-1 S can be traced laterally into the strong negative amplitudes in the NE corner of the Bjørnøya Basin, confined between the uplifted Stappen High and the LFC (Fig. 11A). This location and similar settings thus seem to be key locations for the occurrence of the lower Aptian source rock unit. Furthermore, the Lower Aptian unit in well 7321/9–1 is established to be the most prolific (Table 3). The patchy occurrence of strong negative amplitudes located in the Fingerdjupet Subbasin (Fig. 11A) could potentially indicate local accumulations of organic matter, with similar characteristics to the source rock unit established in well 7321/9–1. However, the Fingerdjupet Subbasin is also one of the most uplifted areas on the SW Barents Shelf (Lasabuda et al., 2021), which further complicate exploration.

The upper Cenomanian organic-rich unit could potentially be a viable option for the wider Tromsø and Bjørnøya basins. However, this unit is absent in the Hammerfest and Bjørnøya basins. The only documented occurrence is in well 7218/11–1 in the transition to the Veslemøy High (Fig. 13B). We therefore suggest that the greatest potential of the upper Cenomanian organic-rich unit is most likely linked to the development off the structural highs, as faulting along their margins developed half-graben depocenters which promoted the formation of restricted marine basins suitable for organic matter to accumulate. A basin wide distribution thus seems unlikely due to the generally well oxygenated waters prevailing the region at these times (e.g. Smelror, 2009).

6. Conclusions

By combining 2D seismic data, amplitude maps and wireline logs with total organic carbon (TOC) and Rock-Eval data, this study documents the presence of four potential source rock units within the Lower Cretaceous succession on the SW Barents Shelf. These are the: (1) upper Hauterivian (2) Barremian, (3) lower Aptian, and (4) upper Cenomanian units. We demonstrate that the deposition and preservation of these units are coupled to localized and restricted fault bound depocenters which developed during multiple episodes of fault activity, mainly attributed to Late Jurassic – Early Cretaceous rifting and local reactivation events along the western Barents Shelf margin.

The Hauterivian and Barremian organic-rich units exhibit TOC contents in the range of 1.0–5.7 wt % and show the greatest potential in the NW part of the Hammerfest Basin. They do not show any potential in the deeper Tromsø and Bjørnøya basins. This is mainly due to deep burial and dilution effects related to regionally high sedimentation rates associated with progradation and the arrival of a large delta system from the west and northwest during the late Albian to Cenomanian times.

The lower Aptian organic-rich unit exhibits TOC contents in the range of 0.57–5.3 wt % and shows the greatest potential by well 7321/9-1 located in the Fingerdjupet Subbasin. It can be traced laterally from this well towards strong negative amplitudes in the central parts of the Fingerdjupet Subbasin, across the Randi Fault Set and further into the southern part of the Fingerdjupet Subbasin. These negative amplitudes may possibly indicate favorable TOC contents, thus resembling the lower Aptian source rock unit in well 7321/9–1, which exhibits high TOC contents (4.0–5.3 wt %). The negative amplitude reflector associated with the lower Aptian source rock unit in well 7321/9–1 can also be traced across from the Fingerdjupet Subbasin into the Bjørnøya Basin, where the unit appears to be composed of kerogen Type III organic matter in the late mature stages (i.e. well 7219/8-1 S). This indicates that the lower Aptian unit could potentially be a viable source rock unit along the Bjørnøyrenna Fault Complex and the Terningen Fault Complex.

The Cenomanian organic-rich unit only appears as an immature, kerogen II-III dominated unit confined to a half-graben situated in the northern part of the Tromsø Basin, at the faulted transition to the Veslemøy High. Correlation towards negative amplitudes located in the deeper basin segments is difficult due to poor well control. Although, the unit can be traced across the Tromsø Basin, there is no indication of a viable source rock of basinal or regional significance.

Declaration of competing interest

The authors declare that they have no known competing financial interests or personal relationships that could have appeared to influence the work reported in this paper.

Acknowledgments

The first author is grateful to WintershallDea Norway for funding this research through a three-year PhD position at UiT - The Arctic University of Norway. This research is also affiliated with the ARCEx consortium (Research Center for Arctic Petroleum Exploration, ARCEx) which is funded by the Research Council of Norway (grant number 228107) and multiple industry partners. The authors are grateful to TGS for allowing to publish their multiclient data. The authors wish to thank reviewers and editors for improving the paper.

Appendix A. Supplementary data

Supplementary data to this article can be found online at https://doi.org/10.1016/j.marpetgeo.2022.105664.

References

Ärlebrand, A., Augustsson, C., Escalona, A., Grundvåg, S.-A., Marín, D., 2021. Provenance, depositional setting and diagenesis as keys to reservoir quality of the Lower Cretaceous in the SW Barents Sea. Mar. Petrol. Geol. 132, 105–217.
Arthur, M.A., Sageman, B.B., 1994. Marine black shales - depositional mechanisms and environments of ancient deposits. Annu. Rev. Earth Planet Sci. 22, 499–551.
Barker, C., 1982. Oil and gas on passive continental margins. In: Watkins, J.S., Drake, C. L. (Eds.), Studies in Continental Margins Geology, vol. 34. American Association of Petroleum Geologists Memoir, pp. 549–565.
Berglund, L.T., Augustson, J., Færseth, R., Gjelberg, J., Ramberg- Moe, H., 1986. The evolution of the Hammerfest Basin. Habitat of hydrocarbons on the Norwegian continental shelf. Proc. conference, Stavanger 319–338.
Blaich, O.A., Tsikalas, F., Faleide, J.I., 2017. New insights into the tectono-stratigraphic evolution of the southern stappen high and its transition to Bjørnøya basin, SW Barents Sea. Mar. Petrol. Geol. 85, 89–105.
Bohacs, K.M., Grabbowski Jr., G.J., Carroll, A.R., Mankiewicz, P.J., Miskell-Gerhardt, K. J., Schwalbach, J.R., Wegner, M.B., Simo, J.A., 2005. Production, destruction, and dilution - the many paths to source-rock development. In: Harris, N.B. (Ed.), The Deposition of Organic-Carbon-Rich Sediments: Models, Mechanisms, and Consequences. SEPM Special Publication No. 82, pp. 61–101.
Bojesen-Koefoed, J.A., Alsen, P., Bjerager, M., Hovikoski, J., Ineson, J., Nytoft, H.P., Nøhr-Hansen, H., Petersen, H.I., Pilgaard, A., Vosgerau, H., 2020. A mid-Cretaceous petroleum source-rock in the North Atlantic region? Implications of the Nanok-1 fully cored borehole, Hold with Hope, northeast Greenland. Mar. Petrol. Geol. 117, 104414. https://doi.org/10.1016/j.marpetgeo.2020.104414.
Bordovskiy, O.K., 1965. Accumulation of organic matter in bottom sediments. Mar. Geol. 3, 33–82.
Bowker, K.A., Grace, T., 2010. The downside of using GR to determine TOC content: an example from the marcellus shale in SE West Virginia. In: Critical Assessment of Shale Resource Plays, AAPG Hedberg Ressearch Conference, Dec., Austin, TX (2010).
Bugge, T., Elvebakk, G., Fanavoll, S., Mangerud, G., Smelror, M., Weiss, H.M., Gjelberg, J., Kristensen, S.E., Nilsen, K., 2002. Shallow stratigraphic drilling applied in hydrocarbon exploration of the Nordkapp Basin, Barents Sea. Mar. Petrol. Geol. 19, 13–37.
Calvert, S.E., Bustin, R.M., Ingall, E.D., 1996. Influence of water column anoxia and sediment supply on the burial and preservation of organic carbon in marine shales. Geochem. Cosmochim. Acta 60, 1577–1593.
Clark, S.A., Glørstad-Clark, E., Faleide, J.I., Schmid, D., Hartz, E.H., Fjeldskaar, W., 2014. Southwest Barents Sea rift basin evolution: comparing results from backstripping and time-forward modelling. Basin Res 26, 550–566.
Cohen, K.M., Finney, S.C., Gibbard, P., Fan, J.-X., 2013. The ICS international chronostratigraphic chart. Episodes 36, 199–204.
Cooper, B.S., Barnard, P.C., 1984. Source rock and oils of the central and northern north sea. In: Demaison, G., Murris, R.J. (Eds.), Petroleum Geochemistry and Basin Evaluation, vol. 35. AAPG Memoir, pp. 303–315.
Corseri, R., Faleide, T.S., Faleide, J.I., Midtkandal, I., Serck, C.S., Trulsvik, M., Planke, S., 2018. A diverted submarine channel of Early Cretaceous age revealed by high-resolution seismic data, SW Barents Sea. Mar. Petrol. Geol. 98, 462–476.
Dalland, A., Worsley, D., Ofstad, K., 1988. A Lithostratigraphic scheme for the Mesozoic and Cenozoic succession offshore mid- and northern Norway. Norwegian Petrol. Direct. Bull. 4.
Demaison, G.J., Moore, G.T., 1980. Anoxic environments and oil source bed genesis. AAPG (Am. Assoc. Pet. Geol.) Bull. 64, 1179–1209.
Demaison, G.J., Hoick, A.J.J., Jones, R.W., Moore, G.T., 1983. Predictive source bed stratigraphy: a guide to regional petroleum occurrence. In: Proceedings of the 11th World Petroleum Congress, vol. 2. John Wiley & Sons, Ltd., London, p. 17.
Doré, A.G., 1995. Barents Sea geology, petroleum resources and commercial potential. Arctic 48, 207–221.
Espitalié, J., Madec, M., Tissot, B., Mennig, J.J., Leplat, P., 1977. Source rock characterization method for petroleum exploration. Paper OTC (Offshore Technology Conference) 2935, 439–444.
Faleide, J.I., Gudlaugsson, S., Jacquart, G., 1984. Evolution of the western Barents Sea. Mar. Petrol. Geol. 1, 123–150.
Faleide, J.I., Vågnes, E., Gudlaugsson, S.T., 1993a. Late mesozoic-cenozoic evolution of the southwestern Barents Sea. Geol. Soc. Lond. Pet. Geol. Conf. Ser. 4, 933–950.
Faleide, J.I., Vagnes, E., Gudlaugsson, S.T., 1993b. Late mesozoic-cenozoic evolution of the south-western Barents Sea in a regional rift shear tectonic setting. Mar. Petrol. Geol. 10, 186–214.
Faleide, J.I., Tsikalas, F., Breivik, A.J., Mjelde, R., Ritzmann, O., Engen, O., Wilson, J., Eldholm, O., 2008. Structure and evolution of the continental margin off Norway and Barents Sea. Episodes 31, 82–91.
Faleide, J.I., Bjørlykke, K., Gabrielsen, R.H., 2015. Geology of the Norwegian continental shelf. In: Bjørlykke, K. (Ed.), Petroleum Geoscience: from Sedimentary Environments to Rock Physics. Springer Berlin Heidelberg, Berlin, pp. 603–637.
Gabrielsen, R.H., Færseth, R.B., Jensen, L.N., Kalheim, J.E., Riis, F., 1990. Structural elements of the Norwegian continental shelf. Part 1: the Barents Sea region. NPD Bull 6, 33.
Gabrielsen, R.H., Grunnaleite, I., Rasmussen, E., 1997. Cretaceous and tertiary inversion in the Bjørnøyrenna Fault complex, south-western Barents Sea. Mar. Petrol. Geol. 14, 165–178.
Gawthorpe, R.L., Leeder, M.R., 2000. Tectono-sedimentary evolution of active extensional basins. Basin Res 12, 195–218.
Grundvåg, S.A., Marin, D., Kairanov, B., Śliwińska, K.K., Nøhr-Hansen, H., Jelby, M.E., Escalona, A., Olaussen, S., 2017. The lower cretaceous succession of the northwestern Barents shelf: onshore and offshore correlations. Mar. Petrol. Geol. 86, 834–857.
Grundvåg, S.A., Jelby, M.E., Sliwinska, K.K., Nohr-Hansen, H., Aadland, T., Sandvik, S.E., Tennvassas, I., Engen, T., Olaussen, S., 2019. Sedimentology and palynology of the Lower Cretaceous succession of central Spitsbergen: integration of subsurface and outcrop data. Norw. J. Geol. 99, 253–284.
Helleren, S., Marín, D., Ohm, S., Augustsson, C., Escalona, A., 2020. Why does not lithology correlate with gamma-ray spikes in the shaley source rocks of the Upper Jurassic Alge Member (southwestern Barents Sea)? Mar. Petrol. Geol. 121, 104–623.
Henriksen, E., Bjørnseth, H.M., Hals, T.K., Heide, T., Kiryukhina, T., Kløvjan, O.S., Larssen, G.B., Ryseth, A.E., Rønning, K., Sollid, K., Stoupakova, A., 2011. Uplift and erosion of the greater Barents Sea: impact on prospectivity and petroleum systems. In: Spencer, A.M., Embry, A.F., Gautier, D.L., Stoupakova, A.V., Sørensen, K. (Eds.), Arctic Petroleum Geology. The Geological Society of London, pp. 271–281.
Herrle, J.O., Schroder-Adams, C.J., Davis, W., Pugh, A.T., Galloway, J.M., Fath, J., 2015. Mid-cretaceous high arctic stratigraphy, climate, and oceanic anoxic events. Geology 43, 403–406.
Ibach, L.E.J., 1982. Relationship between sedimentation-rate and total organic-carbon content in ancient marine-sediments. AAPG (Am. Assoc. Pet. Geol.) Bull. 66, 170–188.
Indrevær, K., Gabrielsen, R.H., Faleide, J.I., 2017. Early Cretaceous synrift uplift and tectonic inversion in the Loppa High area, southwestern Barents Sea, Norwegian shelf. J. Geol. Soc. 174, 242–254.
Isaksen, G.H., Ledje, K.H.I., 2001. Source rock quality and hydrocarbon migration pathways within the greater utsira high area, viking graben, Norwegian north sea. AAPG (Am. Assoc. Pet. Geol.) Bull. 85, 861–883.
Jenkyns, H.C., 1980. Cretaceous anoxic events - from continents to oceans. J. Geol. Soc. 137, 171–188.
Jongepier, K., Rui, J.C., Grue, K., 1996. Triassic to Early Cretaceous stratigraphic and structural development of the northeastern Møre Basin margin, off Mid-Norway. Nor. Geol. Tidsskr. 76, 199–214.
Kairanov, B., Escalona, A., Norton, I., Abrahamson, P., 2021. Early cretaceous evolution of the Tromsø basin, SW Barents Sea, Norway. Mar. Petrol. Geol. 123, 104–714.
Karlsen, D.A., Skeie, J.E., 2006. Petroleum migration, faults and overpressure, part 1: calibrating basin modelling using petroleum in traps – a review. J. Petrol. Geol. 29, 227–256.
Karlsen, D.A., Skeie, J.E., Backer-owe, K., Bjørlykke, K., Ollstad, R., Berge, K., Cecchi, M., Vik, E., Schaefer, R.G., 2004. Petroleum migration, faults and overpressure. Part II. Case history: the Haltenbanken petroleum province, offshore Norway. In: Cubitt, J. M., England, W.A., Larter, S. (Eds.), Understanding Petroleum Reservoirs: towards an Integrated Reservoir Engineering and Geochemical Approach, vol. 237. Geological Society of London Special Publications, London, pp. 305–372.
Katz, B., 2005. Controlling factors on source rock development—a review of productivity, preservation, and sedimentation rate. Soci. Sed. Geol. 82, 7–16.
Kosters, E.C., VanderZwaan, G.J., Jorissen, F.J., 2000. Production, preservation and prediction of source-rock facies in deltaic settings. Int. J. Coal Geol. 43, 13–26.
Langrock, U., Stein, R., Lipinski, M., Brumsack, H.-J., 2003. Late Jurassic to Early Cretaceous black shale formation and paleoenvironment in high northern latitudes: examples from the Norwegian-Greenland Seaway. Paleoceanography 18, 1–16.
Lasabuda, A., Laberg, J.S., Knutsen, S.M., Hogseth, G., 2018. Early to middle Cenozoic paleoenvironment and erosion estimates of the southwestern Barents Sea: insights from a regional mass-balance approach. Mar. Petrol. Geol. 96, 501–521.
Lasabuda, A.P.E., Johansen, N.S., Laberg, J.S., Faleide, J.I., Senger, K., Rydningen, T.A., Patton, H., Knutsen, S.M., Hanssen, A., 2021. Cenozoic uplift and erosion of the Norwegian Barents Shelf-A review. Earth Sci. Rev. 217, 103609.
Leckie, R.M., Bralower, T.J., Cashman, R., 2002. Oceanic anoxic events and plankton evolution: biotic response to tectonic forcing during the mid-Cretaceous. Paleoceanography 17, 1–29.

Leith, T.L., Weiss, H.M., Mørk, A., Århus, N., Elvebakk, G., Embry, A.F., Brooks, P.W., Stewart, K.R., Pchelina, T.M., Bro, E.G., Verba, M.L., Danyushevskaya, A., Borisov, A.V., 1993. Mesozoic hydrocarbon source rocks of the Arctic region. In: Vorren, T.O., Bergsager, E., Dahl-Stamnes, A., Holter, E., Johansen, Å., Lie, Å., Lund, T.B. (Eds.), Arctic Geology and Petroleum Potential. Elsevier, Amsterdam, pp. 1–25.

Lerch, B., Karlsen, D.A., Seland, R., Backer-Owe, K., 2017. Depositional environment and age determination of oils and condensates from the Barents Sea. Petrol. Geosci. 23, 190–209.

Løseth, H., Wensaas, L., Gading, M., Duffaut, K., Springer, M., 2011. Can hydrocarbon source rocks be identified on seismic data? Geology 39, 1167–1170.

Mann, U., Zweigel, J., Øygard, K., Gjeldvik, G., 2002. Source rock prediction in deepwater frontier exploration areas: an integrated study of the Cretaceous in the Vøring Basin. In: Research, S.P. (Ed.), AAPG Hedberg Conference: Hydrocarbon Habitat of Volcanic Rifted Passive Margins, Stavanger, Norway.

Marín, D., Escalona, A., Sliwinska, K.K., Nohr-Hansen, H., Mordasova, A., 2017. Sequence stratigraphy and lateral variability of Lower Cretaceous clinoforms in the southwestern Barents Sea. AAPG (Am. Assoc. Pet. Geol.) Bull. 101, 1487–1517.

Marín, D., Escalona, A., Grundvåg, S.A., Nohr-Hansen, H., Kairanov, B., 2018a. Effects of adjacent fault systems on drainage patterns and evolution of uplifted rift shoulders: the Lower Cretaceous in the Loppa High, southwestern Barents Sea. Mar. Petrol. Geol. 94, 212–229.

Marín, D., Escalona, A., Grundvåg, S.A., Olaussen, S., Sandvik, S., Sliwinska, K.K., 2018b. Unravelling key controls on the rift climax to post-rift fill of marine rift basins: insights from 3D seismic analysis of the Lower Cretaceous of the Hammerfest Basin, SW Barents Sea. Basin Res 30, 587–612.

Marín, D., Helleren, S., Escalona, A., Olaussen, S., Cedeño, A., Nøhr-Hansen, H., Ohm, S., 2020. The Middle Jurassic to lowermost Cretaceous in the SW Barents Sea: interplay between tectonics, coarse-grained sediment supply and organic matter preservation. Basin Res. 33 (2), 1033–1055. https://doi.org/10.1111/bre.12504.

Matapour, Z., Karlsen, D.A., 2017. Ages of Norwegian oils and bitumen based on agespecific biomarkers. Petrol. Geosci. 24, 92–101. https://doi.org/10.1144/petgeo2016–119.

Midtkandal, I., Svensen, H.H., Planke, S., Corfu, F., Polteau, S., Torsvik, T.H., Faleide, J. I., Grundvåg, S.A., Selnes, H., Kurschner, W., Olaussen, S., 2016. The aptian (early cretaceous) oceanic anoxic event (0AE1a) in svalbard, Barents Sea, and the absolute age of the barremian-aptian boundary. Palaeogeogr. Palaeocl. 463, 126–135.

Midtkandal, I., Faleide, J.I., Faleide, T., Serck, C., Planke, S., Corseri, R., Dimitriou, M., Nystuen, J., 2019. Lower Cretaceous Barents Sea strata: epicontinental basin configuration, timing, correlation and depositional dynamics. Geol. Mag. 157, 1–19.

Mitchum, R.M.J., Vail, P.R., Sangree, J.B., 1977. Seismic stratigraphy and global changes of sea-level, part 6: stratigraphic interpretation of seismic reflection patterns in depositional sequences. In: Payton, C. (Ed.), Seismic Stratigraphy – Applications to Hydrocarbon Exploration, vol. 26. Mem. - Am. Assoc. Pet. Geol., pp. 117–133

NPD Factpages, 2021. [WWW Document]. Norwegian Petroleum Directorate. https://factpages.npd.no. (Accessed 3 November 2021).

Ohm, S.E., Karlsen, D.A., Austin, T.J.F., 2008. Geochemically driven exploration models in uplifted areas: examples from the Norwegian Barents Sea. AAPG (Am. Assoc. Pet. Geol.) Bull. 92, 1191–1223.

Øygard, K., Olsen, R., 2002. Alternative source rock in the north atlantic passive Marin – cretaceous in the møre and vøring basins, offshore Norway. AAPG hedberg conference: "hydrocarbon habitat of volcanic rifted passive margins. Stavanger, Norway 1–4.

Parker, J.R., 1967. The jurassic and cretaceous sequence in spitsbergen. Geol. Mag. 104, 487–505.

Pedersen, T.F., Calvert, S.E., 1990. Anoxia vs productivity - what controls the formation of organic-carbon-rich sediments and sedimentary-rocks. AAPG (Am. Assoc. Pet. Geol.) Bull. 74, 454–466.

Peters, K.E., 1986. Guidelines for evaluating petroleum source rock using programmed pyrolysis. AAPG (Am. Assoc. Pet. Geol.) Bull. 70, 318–329.

Peters, K.E., Cassa, M.R., 1994. Applied source rock geochemistry. In: Magoon, L.B., Dow, W.G. (Eds.), The Petroleum System - from Source to Trap. AAPG, pp. 93–120.

Rider, M.H., Kennedy, M., 2011. The Geological Interpretation of Well Logs, third ed. Rider-French, Scotland.

Riis, F., Halland, E., 2014. CO2 storage atlas of the Norwegian Continental shelf: methods used to evaluate capacity and maturity of the CO2 storage potential. Enrgy. Proced. 63, 5258–5265.

Rogov, M.A., Shchepetova, E.V., Zakharov, V.A., 2020. Late Jurassic – earliest Cretaceous prolonged shelf dysoxic–anoxic event and its possible causes. Geol. Mag. 157, 1622–1642. https://doi.org/10.1017/S001675682000076X.

Rønnevik, H., Bescow, B., Jacobsen, H.P., 1982. Structural and Stratigraphic Evolution of the Barents Sea, vol. 8. Canadian Society of Petroleum Geologists Memoir, pp. 431–440.

Sattar, N., Juhlin, C., Koyi, H., Ahmad, N., 2017. Seismic stratigraphy and hydrocarbon prospectivity of the lower cretaceous Knurr sandstone lobes along the southern margin of Loppa high, Hammerfest basin, Barents Sea. Mar. Petrol. Geol. 85, 54–69.

Schlanger, S.O., Jenkyns, H.C., 1976. Cretaceous oceanic anoxic events: causes and consequences. Geol. Mijnbouw 55, 179–184.

Scotese, C.R., Song, H., Mills, B.J.W., van der Meer, D.G., 2021. Phanerozoic paleotemperatures: the earth's changing climate during the last 540 million years. Earth Sci. Rev. 215, 103–503.

Seldal, J., 2005. Lower Cretaceous: the next target for oil exploration in the Barents Sea? Petrol. Geol. Conf. Proceed. 231–240.

Serck, C.S., Faleide, J.I., Braathen, A., Kjølhamar, B., Escalona, A., 2017. Jurassic to early cretaceous basin configuration(s) in the Fingerdjupet Subbasin, SW Barents Sea. Mar. Petrol. Geol. 86, 874–891.

Sheriff, R.E., 2002. Encyclopedic Dictionary of Applied Geophysics, fourth ed. Society of Exploration Geophysicists, Tulsa, Okla.

Smelror, M., Mørk, A., Monteil, E., Rutledge, D., Leereveld, H., 1998. The Klippfisk formation—a new lithostratigraphic unit of Lower Cretaceous platform carbonates on the Western Barents Shelf. Polar Res 17, 181–202.

Smelror, M., Petrov, O.V., Larssen, G.B., Werner, S., Norway, G.S.o., 2009. Geological history of the Barents Sea: atlas. Geological Survey of Norway 1–135.

Sund, T., 1984. Tectonic development and hydrocarbon potential offshore Troms, northern Norway. AAPG (Am. Assoc. Pet. Geol.) Bull. 68, 1206–1207.

Tissot, B.P., Durand, B., Espitalie, J., 1973. Influence of nature and diagenesis of organic matter in formation of petroleum. AAPG (Am. Assoc. Pet. Geol.) Bull. 58, 499–506.

Ulmishek, G.F., 2003. Petroleum geology and resources of the west Siberian Basin, Russia. USGS Bull 1–49, 2201.

Vickers, M.L., Price, G.D., Jerrett, R.M., Watkinson, M., 2016. Stratigraphic and geochemical expression of Barremian-Aptian global climate change in Arctic Svalbard. Geosphere 12, 1594–1605.

White, D.A., 1993. Geologic risking guide for prospects and plays. AAPG (Am. Assoc. Pet. Geol.) Bull. 77, 2048–2061.

Wood, R.J., Edrich, S.P., Hutchison, I., 1989. Influence of North Atlantic tectonics on the large scale uplift of the stapen high and Loppa high, western Barents shelf. In: Tankard, A.J., Balkwill, H.R. (Eds.), Extensional Tectonics and Stratigraphy of the North Atlantic Margins, vol. 46. Mem. - Am. Assoc. Pet. Geol., pp. 559–566

Worsley, D., Johansen, R., kristensen, S.E., 1988. The mesozoic and cenozoic succession of tromsøflaket. In: Dalland, A., Worsley, D., Ofstad, K. (Eds.), A Lithostratigraphic Scheme for the Mesozoic and Cenozoic Succession Offshore Mid- and Northern Norway, vol. 4. NPD Bull., pp. 42–65